

# Review of Developments in Portable Hydrogen Production Using Microreactor Technology

Jamelyn D. Holladay,\* Yong Wang, and Evan Jones

*Battelle, Pacific Northwest Division, Richland, Washington 99352*

*Received January 14, 2004*

## Contents

1. Introduction	4767
2. Reactor Development and Performance Overview	4768
2.1. Fabrication and Design	4769
2.1.1. Materials	4769
2.1.2. Fabrication Techniques	4769
2.1.3. Design Strategies	4770
2.2. Hydrogen Production	4771
2.2.1. Hydrocarbon Reforming	4771
2.2.2. Ammonia Cracking	4773
2.2.3. Other Hydrogen Production Techniques	4773
3. Hydrogen Production from Microreactors	4773
3.1. Subwatt Power	4774
3.1.1. Microreformers (0.01–0.1 W) Developed at Battelle, Pacific Northwest Division	4774
3.1.2. Packed-Bed Microreactor in the Subwatt Power Range	4775
3.1.3. Microscale Preferential Oxidation Reactor	4775
3.2. Power Supplies in the 1–10 W Range	4777
3.2.1. MIT Suspended-Tube Reactor for 1–2 W Power Generation	4777
3.2.2. Lehigh University Methanol Reforming Reactor	4778
3.3. Reactors in the 15–100 W Range	4780
3.3.1. Korea Institute of Energy Research 15 W Power Generation	4780
3.3.2. Battelle, Pacific Northwest Division, 15–100 W Power Generation	4781
3.3.3. MiRTH-e 20–100 W Reactor	4782
3.3.4. Motorola Methanol Fuel Processor	4782
3.3.5. MesoSystems Technology in the 50–100 W Range	4783
3.4. Reactors $\leq$ 500 W	4783
3.4.1. Scalable Methanol Autothermal Reforming Reactor	4783
3.4.2. Portable Power Using a Propane Cracking Reactor System	4783
3.4.3. Methanol Reforming Reactors for a 200 W <sub>e</sub> Fuel Cell Power System	4784
3.4.4. Royal Military College of Canada 200–300 W System	4785
3.4.5. Emission-Free Reformer Concept for Portable Power Applications	4785
4. Summary and Outlook	4786
5. Acronyms	4787
6. References	4787

## 1. Introduction

Technology advancements over time have enabled developments in electronics to move us into a micro-

electronics age. Remarkable achievements have increased functionality while making devices smaller. Each decrease in device size has resulted in greater quality and efficiency. However, as new functionalities are added, power consumption rises alarmingly. Until recently, primary and secondary batteries have been the sole autonomous energy storage solution for these devices, but new and innovative approaches, ranging from microscale rotary engines to thermal electric generators implanted in microscale combustors,<sup>1–6</sup> are laying the groundwork for alternative technologies that generate electric power from hydrocarbon fuels. One innovative way to utilize the stored energy in hydrocarbon fuels is to strip the hydrogen from its compounds and feed it to a fuel cell, producing electricity.

Fuel cell efficiencies and power densities are increasing, while costs are decreasing, making them a potentially attractive power supply.<sup>7–9</sup> Polymer electrolyte membrane fuel cells (PEMFCs) have been proposed as battery replacements and for use in hybrid fuel cell battery systems to augment the battery's energy density.<sup>7–10</sup> However, nontrivial challenges for PEMFCs include hydrogen storage, safety, and water and thermal management.<sup>7,10</sup> One way to avoid the hydrogen storage problem is to produce hydrogen on demand using miniature reactors. These reactors often have characteristic dimensions, such as channel gaps, which are on the microscale (typically  $< 1000 \mu\text{m}$ ) or mesoscale (1000  $\mu\text{m}$  to a few centimeters) and will be referred to in this article as microreactors. These features are significantly smaller than many conventional reactors (a few inches or more), and they can significantly enhance mass and heat transfer rates. Operating on demand, microreactors liberate the hydrogen from hydrogen containing feedstocks such as hydrocarbons, ammonia, or chemical hydrides, as needed, to power the fuel cell. Over the last 30 years, pioneering and follow-up studies have resulted in new concepts and designs for microreactor applications. This paper reviews the progress in microreactor development focused on fuel cell based power supplies ranging from  $< 1 \text{ W}$  to several hundred watts. The discussion first covers reactor types, fabrication and design, and hydrogen production techniques, and then it describes microreactor performance for a wide range of devices.



Jamelyn (Jamie) Holladay received his Master's degree in Chemical Engineering from Brigham Young University in 2000 and has over 4 years of research experience. His work involves microscopic battery design and miniature power supplies using a fuel processor and fuel cell, including microdevice design, heterogeneous catalyst testing, steam reforming, semiconductor processing, PEM fuel cells, and battery fabrication/testing. He is currently contributing to the Sub-Watt Power, Soldier-Portable Power, Soldier-Portable Cooling, and NO<sub>x</sub>/SO<sub>x</sub> emission reduction projects. In addition to technical advancements, these projects also require frequent communications and interactions with industry, military, and educational institutions. He has three patent applications and over 15 peer reviewed publications.



Yong Wang received his Ph.D. in Chemical Engineering from Washington State University in 1993, and he has 20 years of research and project management experience. His main research interest is in the development of advanced catalysts and novel reactors for hydrogen production, natural gas to liquid fuels, alkane conversion to chemicals, solid acid-catalyzed isomerization/alkylation/dehydration, and upgrading of biomass derived feedstocks, as well as in the elucidation of structural and functional relationship on metal oxide based redox and acid/base catalysis. Dr. Wang has received two R&D 100 Awards, a Presidential Green Chemistry Award, and numerous Battelle and PNNL Key Contributor Awards for his contributions. He was named PNNL Inventor of the Year and Battelle Distinguished Inventor in 2003. He has 87 peer reviewed publications, including 28 issued U.S. patents.

## 2. Reactor Development and Performance Overview

Microreactors evolved from the process intensification concepts and microfabrication techniques developed for the microelectronics industry. Process intensification was pioneered in the 1970s, arguably by Imperial Chemical Industries (ICI) researcher Colin Ramshaw, who began developing technologies and approaches that considerably reduced the physical size of unit operations while maintaining their



Mr. Jones has a B.S. and M.S. in Chemical Engineering from Washington State University. His current technical interest is in microscale power systems using small-scale reformer reactors. He has been involved in the design and development of both large and laboratory scale test systems and the development of microtechnology for commercial and government clients. Pilot-plant design has ranged from conceptual P&ID's to final engineering, design, and construction as well as installation and operation. He has designed, constructed, and operated several commercial and pilot-scale systems for manufacturing high-purity chemicals for the electronics industry and recovering acid from metal-bearing spent acids. Mr. Jones has received a R&D 100 Award and a Federal Laboratory Consortium Award, and he has over 15 peer reviewed publications.

throughput.<sup>11,12</sup> Later, the process intensification strategies were combined with microfabrication techniques.<sup>13</sup> Further size reduction was achieved when multiple unit operations, for example, a combustor, heat exchanger, and catalytic reactor, were integrated into a single device.<sup>14,15</sup> The field of microreactors has expanded rapidly over the past decade. By the mid 1990s, a handful of organizations were exploring this reaction technology, including IMM, Forschungszentrum Karlsruhe GmbH (Karlsruhe), DuPont, University of Newcastle, MIT, and the Battelle Pacific Northwest National Laboratory. Today there are dozens of research institutes, universities, and companies actively engaged in the development of microreactors. Microreactors are particularly useful for situations where heat and mass transfer are required for good temperature control, to improve yields or selectivity, or where reactions are only mildly endothermic or exothermic.

For hydrogen production, microreactors offer numerous advantages. High heat and mass transfer rates, for example, enable reactions to be performed under more aggressive conditions which favor overall kinetics or space time yields.<sup>11,13,16</sup> These high rates are due to the high surface-to-volume ratios and short transfer distances in the reactors. For reactions that operate in mass and heat transfer-limited regimes, microreaction devices could be considerably smaller than their conventional counterparts at the same throughput.

There are several challenges that need to be addressed when using the microreactors. Some of these issues include increased sensitivity to fouling, a potentially increased high-pressure drop in the system at high throughput, more difficulty in sealing of the small systems, and increased challenges in system monitoring. Additionally, the high surface area-to-volume ratio allows high heat transfer rates,

**Table 1. Microreactor Material Benefits and Drawbacks (Adapted from refs 17 and 18)**

substrate	benefits	drawbacks
metal	standard fabrication techniques durable low to modest costs no clean room required	poor compatibility with ceramics and glass
silicon	well characterized silicon fabrication techniques high precision low cost	fragile requires a clean room
LTCC	flexible fabrication refractory and durable low cost no clean room required	nonstandard fabrication sealing
polymers	low cost flexible fabrication	chemical compatibility thermal compatibility sealing

which also create more problems in thermal management. Some of these issues (e.g. pressure drop, heat loss, and sealing) can be minimized through the material selection and reactor design. Other issues, such as system monitoring, require other solutions. For example, thermal couples may be a significant source of heat loss in the system, so a solution is to build them in-situ. Many of the researchers have attempted to address these challenges; unfortunately, oftentimes they do not report their methods for overcoming these challenges.

## 2.1. Fabrication and Design

To build an efficient and compact microreactor, the fabrication technique must allow for three-dimensional structures and the use of the appropriate materials, and the technique should be low cost.<sup>13</sup> Since reactants and products must flow in and out of the device, traditional standard thin film techniques are not suitable for the reactor framework. However, thin film techniques are very useful for integration, surface preparation, sensor integration, and finishing or packaging. Fortunately, traditional thin film techniques can be modified for microreactor fabrication; other techniques, which will be discussed below, are also available.

### 2.1.1. Materials

The fabrication materials chosen must be chemically compatible, have the appropriate thermal properties, and be structurally sound. Table 1 lists the benefits and drawbacks of some common materials used in microreactor fabrication. The materials are divided into four general categories: metals, silicon (which includes materials containing silicon or that are processed with semiconductor fabrication techniques), low-temperature cofired ceramics (LTCC), and plastics.<sup>17,18</sup> Polymeric materials would be of great interest in microreactors; however, no hydrogen generating microreactors built of polymers were reported in the literature at the time of this review. It would be an interesting area of development, although the thermal and chemical compatibility may be an issue. The material selection process is complicated by the fabrication process; that is, will the fabrication process alter the material properties and,

if so, how? Microreactors have the potential to be manufactured using high-volume, low-cost techniques, but the design, material, and fabrication selections should take cost into account to avoid developing a laboratory curiosity rather than a commercially viable device.<sup>13</sup>

### 2.1.2. Fabrication Techniques

A number of fabrication techniques meet the general requirements for constructing an efficient and compact microreactor. Popular methods include LIGA, wet and dry etching processes, micromachining, lamination, and soft lithography.

**2.1.2.1. LIGA.** The LIGA technique was primarily developed by researchers in Germany, with Forschungszentrum Karlsruhe and the Institute for Microtechnology Mainz (IMM) being the primary drivers.<sup>19</sup> This process combines deep lithography, electroplating, and molding (lithographie, galvanoformung, abformtechnik—LIGA)<sup>13,19</sup> using three general steps. The first step is the pattern transfer using a serial beam writing process or mask into a photoresist or a special photosensitive epoxy, such as SU8, deposited on an electrically conductive substrate.<sup>13</sup> After any undesirable material is removed (e.g., the mask is developed), a relief structure is formed by electroplating onto the exposed substrate areas. Once the metallic structure is formed, the resist or epoxy is removed. In some instances, this metallic structure may be the final product; however, usually it is used as a master tool for a replication process (such as injection molding, casting, or embossing), which is the final step in the process.<sup>13,19</sup>

**2.1.2.2. Wet and Dry Etching Processes.** Wet and dry etching processes have largely been developed for the semiconductor industry. Wet etching uses a liquid etch solution (such as potassium hydroxide to etch silicon) to remove unwanted material from the substrate anisotropically, whereas dry etching tends to use plasmas or reactive plasmas and may be anisotropic or isotropic, depending on the plasma source.<sup>13</sup> Similar to dry etching is deep reactive ion etching (DRIE), which is often used in the fabrication of microelectromechanical systems (MEMS).<sup>19</sup> Since wet etching is an anisotropic process, it has strong restrictions on the geometries that can be made. Isotropic dry etching enables a wider variety of geometries but is more limited in the materials that can be etched. The initial step in the process is the same as that of LIGA; specifically, a pattern is transferred into a photoresist or other protective layer. The unprotected substrate areas are etched using either technique. Next, the protective layer is removed. To make the final device, several substrates fabricated using this method are stacked on top of each other.<sup>13</sup>

**2.1.2.3. Micromachining.** In contrast to LIGA and wet/dry etching, the three main processes for micromachining shapes typically do not need the initial deposition of a resist, epoxy, or other protective layers. The equipment also tends to be less expensive for purchasing and maintenance. While not required, these processes are often computer controlled. The first technique involves traditional milling, turning,

and grinding, but with ultraprecision machines that produce small features.<sup>13,19</sup> The feature sizes are not as small as those constructed from LIGA and other fabrication processes; however, almost any material can be used. The second technique uses laser radiation to remove material or, in some situations, to build up material.<sup>13</sup> The most common procedure is to remove material by melting, evaporation, decomposition, photoablation, or a combination of these removal techniques. Some development involves building structures by photochemically cross-linking in organic compounds or powder solidification by laser sintering. Both processes can be used to make devices down to critical dimensions of approximately 10  $\mu\text{m}$ ; however, the surfaces tend to be rough, which may cause problems in some cases.<sup>13</sup> The third technique is electrodischarge machining (EDM), also called micro-electrodischarge machining. This technique is limited to electrically conductive work pieces. Material is removed by small sparks in a dielectric fluid, such as deionized water or oil, between the work piece and an electrode. The main disadvantages of this type of machining are relatively rough surfaces; limitations in miniaturization to the size of the electrodes and spark; and relatively long machining times, which may limit the technology to prototyping and manufacture of mold inserts.<sup>13</sup>

**2.1.2.4. Lamination.** In a lamination process, several sheets with different patterns are stacked and then brazed or bonded together. In a MEMS-based approach, DRIE is used to make patterns in silicon or other materials. The substrates are then stacked and bonded together using silicon bonding methods developed for MEMS. Another approach, used by researchers at Pacific Northwest National Laboratory (PNNL),<sup>19</sup> is the fabrication of thin metal laminates using stamping, embossing, or processes described previously. These laminates are then stacked and brazed or diffusion bonded into a single device.<sup>19–21</sup> Lamination is also particularly well suited for fabricating ceramic devices. Ceramic tapes, in the soft, pliable “green state”, are cut, molded, laser cut, and so forth to the desired design and stacked. After curing in high-temperature furnaces, the laminates are bonded into a single structure.<sup>19</sup>

**2.1.2.5. Soft Lithography.** Whitesides and co-workers developed a collection of lithographic techniques referred to as soft lithography.<sup>21</sup> An elastomer, often poly(dimethylsiloxane), with a pattern embossed on its surface, is used to transfer the pattern onto the substrate (often by stamping). This technique is used in biological applications but can be combined with other polymers, electroplating techniques, or molding of ceramics for low-cost, fast prototyping of devices.<sup>19,21</sup>

### 2.1.3. Design Strategies

Various reactor types have been used as the foundation for microreactor designs, including coated wall reactors, packed-bed reactors, structured catalyst reactors, and membrane reactors.

**2.1.3.1. Coated Wall Reactors.** Techniques for depositing catalyst onto the reactor walls include

wash coating, ink jet printing, aerosol sprays, and thin film deposition by chemical or physical vapor deposition.<sup>19</sup> Wash coating techniques, similar to those used in conventional autoconverter manufacturing, can form a thin layer of catalyst with high surface area on reactor walls which results in more efficient utilization of catalysts compared to their conventional counterparts such as pellets or extrudates. Unfortunately, due to nonuniform surface tension, the wash coating solutions tend to collect in the corners of the reactors.<sup>19</sup> However, in some cases, the surface tension phenomenon can be an advantage, as demonstrated, for example, by the innovative work of Arana et al.,<sup>22</sup> who used surface tension to make a stop valve to control catalyst deposition.

With aerosol sprays, the catalyst is deposited directly on the reactor substrate, and the sprays can be used to coat already-formed channels.<sup>19</sup> Ink jet catalyst ink deposition allows precise placement of the catalyst, but at the cost of having to seal the system after deposition, which eliminates some fabrication options such as diffusion bonding. Additionally, the choice of catalyst composition allowed by ink deposition is limited. Physical or chemical vapor deposition techniques place thin catalyst layers with low surface areas. Examples of these techniques include electron beam deposition, radio frequency (RF) sputtering, thermal vaporization, chemical vapor deposition (CVD), and reactive chemical vapor deposition. These resulting smooth surfaces can be roughened by thermal activation to increase their surface area, but surface areas similar to those for wash coating generally cannot be attained. With physical deposition, as with sputtering, it is difficult to achieve uniform coating on nonplanar surfaces. Additionally, both methods are typically limited to metals and simple oxides due to the availability of precursors.

**2.1.3.2. Packed-Bed Microreactors.** Packed-bed microreactors simply pack conventional catalysts in microreactors. The advantages of using conventional catalysts include decreased cost, increased catalyst availability and reproducibility, and greater understanding of catalyst performance. The high heat and mass transfer rates in microreactors tend to boost the performance of these catalysts.<sup>19</sup> The disadvantages of the packed-bed reactors include a high-pressure drop and potential channeling at high throughput, and the possibility of channel plugging.<sup>19</sup>

**2.1.3.3. Structured Catalyst Reactors.** The powder used in packed-bed reactors can be integrated onto a foam or felt substrate to be used in microreactors.<sup>23</sup> By supporting the catalyst on structured substrates, plugging can be avoided and pressure drop can be reduced due to the large opening pores in the foams or felt (typically 100–300  $\mu\text{m}$  in diameter). Additionally, conventional catalysts typically used in packed-bed reactors can be used, which offers a much wider range of catalyst availability with high reproducibility. This type of reactor often consists of narrow microchannels, where the supported catalysts are placed. Problems associated with “channeling” can be mitigated by designing channel geometries such that the laminar average residence time is

longer than the radial diffusion time. Fast mass transfer rates can be achieved with this design.<sup>24</sup>

A variation of this technique was developed by Wan et al.<sup>25</sup> to grow zeolites in microchannels. The first step was to place seed in the channel(s) where the zeolite was desired. Once the seed was in place, zeolites could be grown using conventional techniques, with the deposition steps repeated a number of times to obtain the desired thickness. These zeolites could be coated or further patterned with photoresist and buffered oxide etch. Once the desired pattern was achieved, the photoresist was stripped using acetone. Free-standing zeolite membranes were also fabricated using this technique with the additional step of silicon etching using tetramethylammonium hydroxide. Wan et al.<sup>25</sup> fabricated films of ZSM-5 and titanium silicate-1.

**2.1.3.4. Membrane Reactors.** Membrane separation techniques are a common way of obtaining high-purity (often  $\geq 99.99\%$ ) hydrogen in industry. For small reactors, it is appealing to combine the hydrogen purification step with the generation reactors to make compact devices.<sup>19</sup> Metal membranes, typically palladium or palladium alloys, are used in these reactors. In conventional systems, high pressures (often greater than 250 psi) and temperatures of 300 °C or more are required for high hydrogen recovery.<sup>26</sup> The small feature sizes and complex geometries possible in microreactors have enabled extremely thin metal membranes to be fabricated that allow high hydrogen recovery at relatively low pressures.<sup>19</sup>

## 2.2. Hydrogen Production

Four hydrogen production techniques are reviewed: hydrocarbon reforming; ammonia cracking; and two other, less common, production techniques, pyrolysis and aqueous phase reforming.

### 2.2.1. Hydrocarbon Reforming

The majority of microreactors currently being developed are designed to produce hydrogen from hydrocarbons. Three basic reforming technologies are steam reforming, partial oxidation, and autothermal reforming. Endothermic steam reforming of hydrocarbons, favored by industry, operates at high temperatures and requires an external heat source. Partial oxidation is an alternative to steam reforming, where the reaction heat is provided by the partial combustion of the hydrocarbon with oxygen. The autothermal reforming process is a thermally neutral hybrid of steam reforming and partial oxidation. All three processes are typically coupled to the shift reactions carried out in the presence of an iron catalyst at about 350 °C and/or a copper catalyst at lower temperatures (210–330 °C) to ensure high yields of hydrogen. Partial oxidation and autothermal processes do not require an external heat source, but an expensive and complex oxygen separation unit is needed (or the hydrogen is diluted with nitrogen, which lowers the fuel cell efficiency). A brief overview of hydrocarbon reforming is given here. Recent articles<sup>28–30</sup> provide a more in-depth review on hydrocarbon reforming for fuel cells.

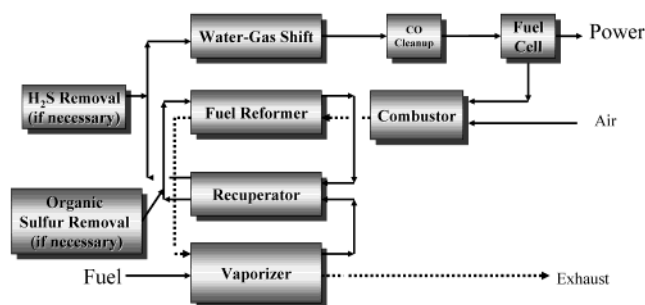


**Figure 1.** Schematic of fuel reforming process.

Steam reforming is generally the preferred process for hydrogen production.<sup>27</sup> Particularly for portable hydrogen production, the requirement of an external heat source can be addressed through the advanced heat and mass transfer provided by microreactors.

Logistic fuels, such as jet and diesel fuels, are readily available, but a compact and effective way to remove sulfur from these fuels is needed for portable hydrogen production. Consequently, for most portable applications, it is likely that sulfur-free fuels, such as methanol, will be used. An additional advantage of methanol is that it is easier to activate at low temperatures than other hydrocarbons. Therefore, a portable hydrogen production unit based on methanol steam reforming would be simpler and less costly than other alternatives. Methanol can also be considered an energy carrier as an alternative to liquefied natural gas.

Methanol steam reforming takes place over Cu or Pd/Zn alloy catalysts<sup>26,31–38</sup> at low temperatures, typically above 200 °C. Low temperature reduces the equilibrium CO selectivity via the water-gas-shift (WGS) reaction. Therefore, a methane-free hydrogen can be produced at low temperatures and high pressures, while near complete conversion to CO<sub>2</sub> can be achieved. The major disadvantage with Cu-based catalysts is the sintering of metal at temperatures above 330 °C, which is difficult to avoid when part of the methanol is combusted to provide heat for the endothermic methanol steam reforming. Pd/Zn alloy catalysts,<sup>32,36,39,40</sup> on the other hand, exhibit excellent thermal stability and are nonpyrophoric and, thus, are an advantage for portable hydrogen production.<sup>41</sup> A schematic of the process is shown in Figure 1. For PEM fuel cells, the carbon monoxide levels need to be below 10 ppm; therefore, secondary WGS reactors and a final polishing step (selective partial oxidation or methanation) are typically used.<sup>26,30,42</sup> In the cases where methanol steam reforming is performed or a metal membrane is used to purify the hydrogen,<sup>26</sup> the WGS can be eliminated.

As with the other reactor configurations, vaporizers, heat exchangers, and a heat source are also needed for microreactors.<sup>26,30,42</sup> Unless the hydrogen is 99.999% pure, the PEM fuel cell typically will utilize 70–80% of the diluted hydrogen fed to it. The unreacted hydrogen from the fuel cell anode, augmented with additional fuel as needed, can be used as fuel for the combustor.<sup>26</sup> The use of anode off-gas requires special controls for transient operating conditions; for example, a mechanism is needed to

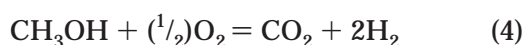
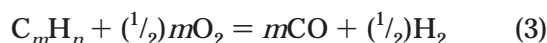
prevent the system from unexpected cooling if the load to the fuel cell is suddenly increased or if the fuel cell hydrogen consumption increases. The system can overheat when the load to the fuel cell is removed, and excess hydrogen is then sent to the combustor.

The reforming, WGS, and oxidation reactions can be generalized as follows for hydrocarbon and methanol fuels:

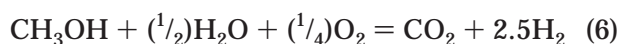
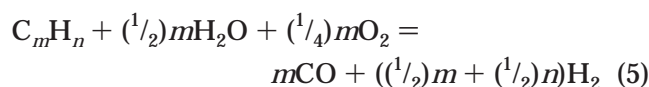
#### Steam reforming



#### Partial oxidation



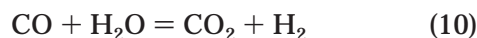
#### Autothermal reforming



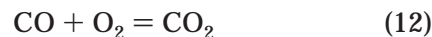
#### Carbon formation



#### Water-gas-shift



#### CO oxidation



Fuel processing reactors are designed to maximize hydrogen production reactions (eqs 1–6 and 10–12) by optimizing the operating conditions and designing the specific catalysts. Under certain conditions, undesirable reactions (eqs 7–9 and 13) will occur.<sup>26,30,42</sup>

Fuel processing occurs at essentially two different temperature ranges and uses several different types of catalysts.<sup>26,30,42</sup> Fuel reforming of fuels other than methanol requires temperatures typically greater than 500 °C. The catalysts can be divided into two types: nonprecious metal (typically nickel) and the noble group 8 metals (typically platinum or rhodium based). Conventional steam reformers have severe mass and heat transfer limitations, and the effectiveness factor of the catalyst is typically <5%.<sup>43</sup> Therefore, the activity of the catalyst is rarely a limiting factor with conventional reactors,<sup>28</sup> and because of their moderate cost, nickel catalysts are used universally in industries. In the case of microreactors

for steam reforming where the intrinsic kinetics of steam reforming can be exploited,<sup>24</sup> the noble group 8 metals, particularly Rh,<sup>44</sup> are preferred, since they exhibit much higher specific activities than nickel catalysts.<sup>45,46</sup> The high temperatures required for reforming hydrocarbons promote carbon formation; by adding water, the coke formation is decreased. Stoichiometric steam-to-carbon ratios are not sufficient to prevent coke formation. Therefore, ratios higher than the stoichiometry, typically 2.5 or greater, are required to gasify coke and are typically used. Coke formation is much less over the noble group 8 metals. Alkaline components such as magnesia or potassia are added to the catalyst support to minimize the coke formation.<sup>47</sup>

Direct partial oxidation of hydrocarbons and catalytic partial oxidation of hydrocarbons are being used in many of the larger-scale hydrogen production systems for automobile fuel cells.<sup>29</sup> The noncatalytic partial oxidation of hydrocarbons in the presence of oxygen and steam typically occurs with flame temperatures of 1300–1500 °C to ensure complete conversion and to reduce soot formation.<sup>28</sup> Catalytic partial oxidation is being used to lower the operating temperatures; however, it is proving hard to control because of coke and hot spot formation due to the exothermic nature of the reactions.<sup>30,42</sup> Krummenacher et al.<sup>48</sup> have had success using catalytic partial oxidation for decane, hexadecane, and diesel fuel. The high operating temperatures (>800 °C and often >1000 °C)<sup>48</sup> may make their use for practical portable devices difficult due to thermal management. Autothermal reforming couples steam reforming with catalytic partial oxidation. Partial oxidation or catalytic partial oxidation is used to generate the heat needed to drive the steam reforming reactions in this process. Many of the technical issues of this type of reforming are discussed by Krumpelt and Bellows.<sup>49–51</sup>

Since carbon monoxide is a poison to PEM fuel cells, it must be reduced to 10 ppm or lower. This can be done by using a metal membrane, as described previously, or catalytically using preferential oxidation or methanation. For fuels other than methanol, the product gas from a reformer contains high amounts of carbon monoxide, often 10% or more.<sup>26,30,42</sup> A WGS reactor is used to reduce the carbon monoxide and also increase the hydrogen production. A high temperature is desired to achieve fast kinetics but results in high carbon monoxide selectivity due to equilibrium limitations. Therefore, a low-temperature reactor is used to lower the carbon monoxide content to 1% or less. TeGrotenhuis et al.<sup>52</sup> have demonstrated the potential in using microreactors to build a gradient-temperature WGS reactor that contains the high-temperature WGS and low-temperature WGS in a single unit for >2–3 kW<sub>e</sub> units. The most common catalyst for WGS is Cu based,<sup>26,30,42</sup> although some interesting work is currently being done with molybdenum carbide,<sup>53</sup> platinum based catalysts,<sup>54,55</sup> and Fe–Pa alloy catalysts.<sup>56</sup>

To further reduce the carbon monoxide, a preferential oxidation reactor or a carbon monoxide selective methanation reactor is used.<sup>26,30</sup> The term “selective oxidation” is also used for preferential oxi-

dation, but more specifically, it refers to cases where carbon monoxide reduction occurs within the fuel cell.<sup>26</sup> The preferential oxidation reactor increases the system complexity because carefully measured concentrations of air must be added to the system.<sup>26,30</sup> However, these reactors are compact, and if excessive air is introduced, some hydrogen is burned. Methanation reactors are simpler in that no air is required; however, for every carbon monoxide reacted, three hydrogen molecules are consumed. Also, the carbon dioxide reacts with the hydrogen, so careful control of the reactor conditions needs to be preserved in order to maintain the selectivity. Therefore, preferential oxidation is currently the primary technique being developed.<sup>26</sup> The catalysts for both these systems are typically noble metals such as platinum, ruthenium, or rhodium supported on Al<sub>2</sub>O<sub>3</sub>.<sup>26,30</sup>

### 2.2.2. Ammonia Cracking

Ammonia is an inexpensive and convenient method of storing hydrogen and may be very suitable for portable power applications.<sup>57</sup> Pure ammonia has a lower heating value (LHV) of 8.9 (kW h)/kg, which is higher than that of methanol (6.2 (kW h)/kg) but less than that of diesel or JP8 (13.2 (kW h)/kg).<sup>58</sup> Up to about 30 vol % of ammonia can be dissolved in water.<sup>57</sup> Unfortunately, ammonia is very toxic and its toxicity may make it difficult to establish a suitable infrastructure to distribute it in a concentrated solution. Proponents quickly point out that ammonia's strong odor makes leak detection simple, reducing some of the risk.<sup>57</sup> The most significant advantage for ammonia is the simplicity of the gas clean up step, since it decomposes into hydrogen and nitrogen. The only gas cleanup required is removal of any unreacted ammonia from the product stream.<sup>57</sup> Ammonia removal in the stream prior to the PEMFC is essential, since, unlike reversible losses from carbon monoxide exposure, long exposure to ammonia (e.g., >15 h) causes severe and irreversible losses in performance.<sup>59</sup>

Endothermic ammonia cracking is regarded as the reverse of the synthesis reaction, and since it is limited by heat transport, its efficiency can potentially be improved using microreactors. In industry, ammonia synthesis occurs at approximately 500 °C and 250 atm, and it is often represented by the following reaction:<sup>57</sup>

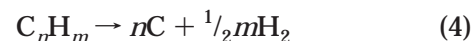


Typical catalysts used in both ammonia synthesis and cracking include iron oxide, molybdenum, ruthenium, and nickel. Unlike synthesis, cracking does not require high pressures, and typically it operates at temperatures around 800–900 °C.<sup>57</sup>

### 2.2.3. Other Hydrogen Production Techniques

Two other hydrogen production methods, pyrolysis and aqueous reforming, have been explored for use in microreactors. Pyrolysis is the decomposition of hydrocarbons into hydrogen and carbon in water-free and air-free environments.<sup>60</sup> If no water or air is present, no carbon oxides (e.g., CO or CO<sub>2</sub>) are

formed. Consequently, this process offers significant emissions reduction. Since no CO or CO<sub>2</sub> is present, secondary reactors are not necessary. However, if air or water is present, then significant CO<sub>2</sub> and CO emissions will be present. Among the advantages of this process are fuel flexibility, relative simplicity and compactness, a clean carbon byproduct, and reduction in CO<sub>2</sub> and CO emissions.<sup>60</sup> The reactions can be written in the following form:<sup>60</sup>



Typical unit operations required for this system include vaporizers/preheaters, a pyrolysis reactor, and recuperative heat exchangers. One of the challenges with this approach is the potential for fouling by the carbon formed, which is particularly important in microreactors.

An aqueous phase can also be used to reform or process hydrocarbon fuels or carbohydrates.<sup>61,62</sup> These reactors often operate at pressures up to 25–30 MPa and temperatures up to 500–750 °C. The advocates of this technology claim that the small characteristic sizes of microreactors more easily accommodate high pressures than larger reactors. The high pressures, in turn, enable the reactors to be even smaller while maintaining the same production rates. However, the balance-of-plant (BOP) components may be difficult to find, depending on the size. In addition, these reactors tend to be large due to low space time yields and in reality do not have a characteristic dimension in the micro or meso range, so they are not reviewed in detail in this paper.

## 3. Hydrogen Production from Microreactors

Numerous groups using multiple methods have developed microreactors for hydrogen production. These microreactors are discussed, beginning with low-power subwatt production reactors and progressing to the larger units. In general, there are very few references describing the performance of complete micropower systems. Consequently, very few authors report system efficiencies, or if reported, these efficiencies are estimates based on the assumed performance of other components, such as pumps, valves, control systems, and fuel cells. Furthermore, the efficiency of the microscale balance of equipment tends to be lower than that of conventional, larger-scale versions. Fortunately, work is being conducted to improve the microscale balance of equipment, which will in turn improve system efficiencies.

With respect to microscale reactors that produce up to several watts of output, the primary loss of efficiency is from thermal losses. Reformer reactors have areas that reach temperatures above 300 °C, and consequently, loss by conduction can be significant. While microscale systems can have advantages over commercial reactors, one disadvantage is the potential for heat loss by conduction through the relatively large tubing and piping connected to the miniature reactors. The instruments and piping connected to a large-scale reactor represent an insignificant heat loss due to their small size relative to the reactor. However, in a microscale system, the



**Figure 2.** Battelle subwatt power microreformers. (Reprinted with permission from ref 41. Copyright 2002 Elsevier.)

tubing and instruments connected to the microscale reactor are relatively large and represent a significant potential for heat loss.

### 3.1. Subwatt Power

#### 3.1.1. Microreformers (0.01–0.1 W) Developed at Battelle, Pacific Northwest Division

Researchers at Battelle, Pacific Northwest Division (Battelle), are developing a methanol reformer for use in subwatt power supplies.<sup>41,63–69</sup> These reformers were originally designed to operate with high-temperature fuel cells developed and fabricated by Case Western Reserve University.<sup>69</sup> A complete system incorporates two vaporizers/preheaters, a heat exchanger, a catalytic combustor, and a catalytic methanol reformer in a volume <0.25 cm<sup>3</sup> and weighing <1 g.<sup>41,66,69</sup> These systems, intended for use in micro-sensors and other MEMS devices, were designed to provide <1 W of power. The reformers were fabricated using conventional milling techniques from stainless steel. In addition to the original design, second-generation designs focused on a high-efficiency processor and a low carbon monoxide design that included a selective carbon monoxide methanation reactor for CO cleanup (Figure 2). The initial reactor had a small methanol reformer reactor with a volume of <5 mm<sup>3</sup>.<sup>41</sup> The second-generation, higher-efficiency design had a larger methanol reforming reactor and smaller heat recuperator heat exchanger, which maintained the original small volume.<sup>66</sup> The

selective carbon monoxide methanation reactor incorporated into the device to lower the CO levels increased the volume, although it was still <0.25 cm<sup>3</sup>.<sup>66</sup> The processor temperature was monitored by a 0.01 in. thermocouple inserted into the catalytic combustion chamber.<sup>41</sup>

The reformers were operated without any external heating, even during startup.<sup>41</sup> The combustion fuel was either hydrogen or methanol, depending on the experiments. The startup procedure consisted of feeding a hydrogen–air mixture to the combustor at room temperature. The hydrogen combustion on the catalyst surface would heat the reactor to 70–100 °C. At these temperatures, methanol could be fed to the vaporizers as the combustion fuel. When methanol was to be the only fuel, the amount of hydrogen would be decreased as the combustion of methanol proceeded.<sup>41</sup> The combustor reactor was operated at 250–450 °C, with typical methanol flow rates of 0.2–0.4 cm<sup>3</sup>/h and air flow rates of 15–25 sccm.<sup>41,63–70</sup>

The reformer performance is shown in Table 2. The fuel for the original reactor was a 50 wt % mixture of methanol and water. For the higher-efficiency reactor and the system that included carbon monoxide cleanup, the fuel mixture was 60 wt % methanol in water.<sup>41,66,69</sup> The efficiency was calculated using the following equation:

$$\text{efficiency} = \frac{\Delta H_c(\text{hydrogen produced})}{\Delta H_c(\text{methanol feed}) + \Delta H_c(\text{fuel feed})} \quad (5)$$

where  $\Delta H_c$  is the lower heating value of the indicated components.<sup>64</sup>

The increase in efficiency between the first- and second-generation reactors was attributed to less water in the feed and lower operating temperatures.<sup>67</sup> Reactor models indicated that the major source of heat loss was by thermal conduction. The selective methanation reactor lowered the carbon monoxide levels to below 100 ppm, but at the cost of some efficiency. The lower efficiency was attributed to slightly higher operating temperatures and to hydrogen consumption by the methanation process. Typical methane levels in the product stream were 5–6.2%.<sup>67</sup>

**Table 2. Battelle Subwatt Power Microscale Fuel Processor Performance<sup>a</sup>**

feed rate (cm <sup>3</sup> /h)	<i>T</i> (°C)	reformate flow (sccm)	hydrogen (%)	carbon monoxide (%)	carbon dioxide (%)	thermal efficiency (%)
0.05	400	1.1	Original Processor <sup>63</sup>			
			73–74	1.0–2.0	25–26	9
0.05 0.08 0.12 0.15 0.18 0.20	255 263 270 280 313 320	1.2 2.0 3.0 3.8 4.5 4.9	High-Efficiency Processor <sup>63</sup>			
			73–74	0.4–0.6	25–26	15
			73–74	0.5–0.7	24–26	21
			73–74	0.5–0.6	25–26	25
			72–73	0.6–0.7	25–27	28
			72–73	0.8–1.0	25–26	30
			72–73	1.0–1.1	25–26	33
0.05 0.08 0.10 0.15	304 323 330 345	1.0 1.65 2.1 3.2	High-Efficiency Processor with Carbon Monoxide Cleanup <sup>63</sup>			
			69–70	<0.01	25–25.5	9.5
			69–70	<0.02	25–25.5	14
			69–70	<0.02	25–25.5	17
0.15	345	3.2	68–69	<0.03	25–26	19

<sup>a</sup> Methanol conversion > 99%. Data adapted from refs 41 and 63–70.

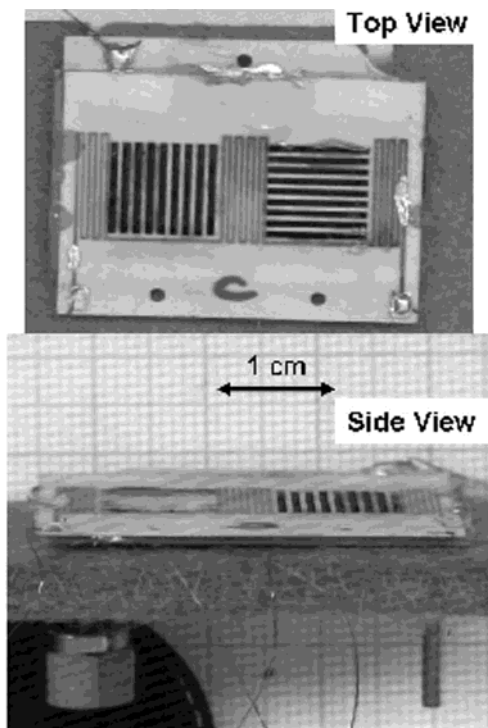


**Figure 3.** Mesoscale fuel cell fabricated by Case Western Reserve University. (Reprinted with permission from ref 63. Copyright 2001 Elsevier.)

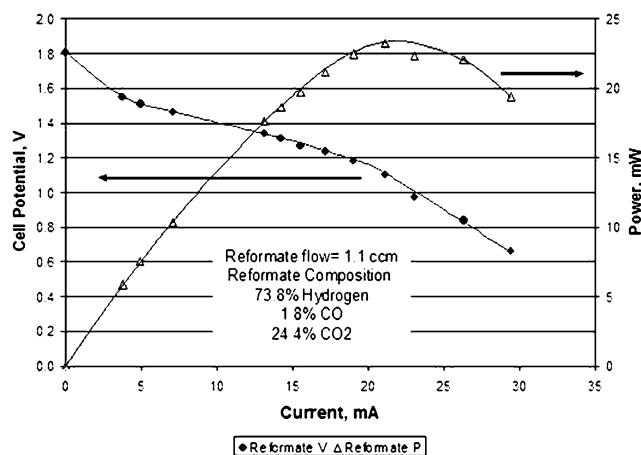


**Figure 4.** Performance of the mesoscale fuel cell and Battelle's microscale methanol processor. (Reprinted with permission from ref 63. Copyright 2001 Elsevier.)

A mesoscale high-temperature fuel cell was operated using the reformat from the original reactor.<sup>69</sup> This fuel cell utilized phosphoric acid doped polybenzimidazole (PBI) technology and was fabricated using an amalgamation of conventional and microfabrication techniques (Figure 3). The PBI technology enabled it to operate at temperatures  $> 125$  °C. At these temperatures, the fuel cell can tolerate high levels of carbon monoxide ( $\approx 2\%$ ) while maintaining sufficient ionic conductivity for proper fuel cell operation.<sup>69</sup> Over 20 mW<sub>e</sub> of power was produced from the integrated methanol processor and fuel cell (Figure 4).<sup>69</sup> Data from fuel cell testing with the other methanol processors have not been reported. In addition, long-term durability and thermal cycling



**Figure 5.** Miniature reformer showing the evaporator, superheater, reactor, and gas collection insert. The catalyst in the picture is in powder form.<sup>37</sup>

testing need to be done on both the fuel processor and the fuel cell.

### 3.1.2. Packed-Bed Microreactor in the Subwatt Power Range

Researchers from the University of Toledo, Case Western Reserve University, the NASA Glenn Research Center, and the National Center for Microgravity Research are collaborating to develop a microreactor consisting of an evaporator, a superheater, a reactor bed, and a "gas collector" within a volume of 1.86 cm<sup>3</sup> (Figure 5).<sup>37</sup> This cylindrical reactor was built from borosilicate glass. Heat for the processor was provided by Kanthal wire resistance heaters wrapped around the outside of the processor. The reactor was designed for methanol reforming and utilized a commercial (Sud-Chemie C18-07-01) Cu/ZnO on Al<sub>2</sub>O<sub>3</sub> support in a powder or pellet form. Figure 5 illustrates the device loaded with a powder catalyst. The device contains 35–50% Cu and 40–55% ZnO with added components to improve its stability. The researchers believe that the Cu/ZnO catalyst not only reforms methanol but also operates as a water-gas-shift (WGS) catalyst. For the experiments, the reactor was loaded with approximately 0.118 g of catalyst powder or 10 catalyst pellets, each with a diameter of 0.48 cm, a thickness of 0.24 cm, and a total mass of 1.14 g.<sup>37</sup>

The processor was operated at atmospheric pressure and at 117–130 °C or 200 °C. A methanol–water mixture (1:1.5 molar ratio) was fed at 0.1 cm<sup>3</sup>/h using a syringe pump. The reactors loaded with powder and pellets had comparable results, but the researchers preferred the powder packed bed form for its smaller volume and mass. The best hydrogen production was obtained at low temperatures, providing, on a dry gas basis, 70% hydrogen, 0.5% carbon monoxide, and residual carbon dioxide. Methanol conversion or thermal efficiency was not reported.<sup>37</sup>

### 3.1.3. Microscale Preferential Oxidation Reactor

As mentioned earlier, reformat from a fuel processor often needs addition processing to reduce the carbon monoxide levels. Researchers at the Stevens Institute of Technology are developing a microscale preferential oxidation (PrOx) reactor to decrease the carbon monoxide level in the reformat stream to below 100 ppm. As part of their research, they used advanced computational fluid dynamic modeling,

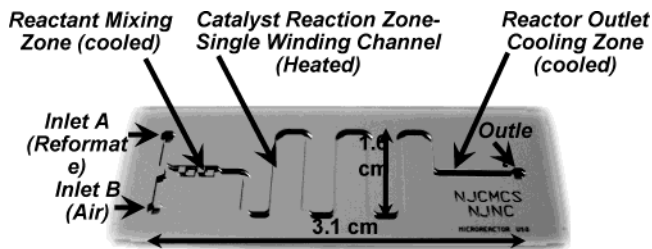


**Figure 6.** Silicon microreactor for preferential oxidation of CO designed for a 0.25  $W_e$  fuel cell. (The researchers wish to express their gratitude to DARPA for funding Grant N66001-02-1-8942.)

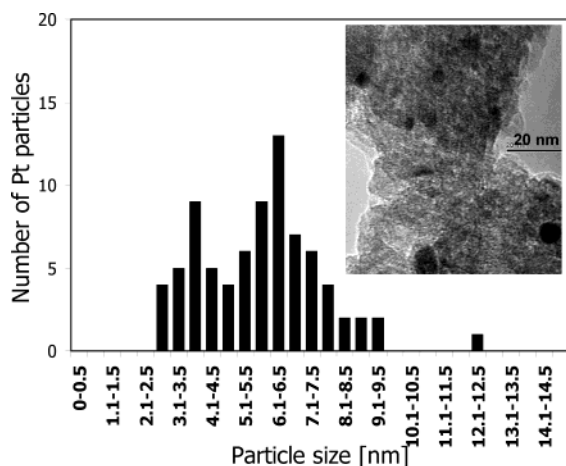


**Figure 7.** Pt particles' size distribution obtained from TEM on  $Al_2O_3$  support with a TEM image of the catalyst. (The researchers wish to express their gratitude to DARPA for funding Grant N66001-02-1-8942.)

microfabrication to build the reactor, and advanced kinetic modeling to understand their experimental results.<sup>33,71–78</sup>

Microscale chemical reactors were successfully fabricated on p-type <100> 8 in. silicon wafers by using state-of-the-art silicon bulk micromachining techniques. The microchannels were formed by DRIE.<sup>76</sup> The reactor consists of dual gas inlets, a mixing region, and a single reaction channel with an outlet (Figure 6).<sup>74</sup> The microreactor shown in Figure 6 has a channel that is 4.5 cm long, 500  $\mu m$  wide, and 610  $\mu m$  deep. The effectiveness of the mixer was confirmed by simulation in FLUENT.

Platinum supported on an alumina catalyst was used in this reactor. The precursor was synthesized using a sol-gel technique.<sup>71</sup> The support, after calcination at 500  $^{\circ}C$ , showed a high specific surface area of 400  $m^2/g$ .<sup>33,72</sup> Transmission electron microscopy (TEM) was used to determine that the platinum particles appeared to have a spherical shape and were evenly distributed on the  $Al_2O_3$  support (Figure 7).<sup>33,72</sup> The platinum particle size distribution was in the range 2.5–8 nm and showed an indication of a bimodal distribution.<sup>33,72</sup> The mean Pt particle size was calculated from the X-ray diffraction (XRD) pattern and was found to be 11 nm, while CO chemisorption gave an average particle size of 6 nm, confirming the particle size distribution obtained from TEM.<sup>33,72</sup>

The general procedure of depositing the catalyst into the reactor is to infiltrate the microchannel with

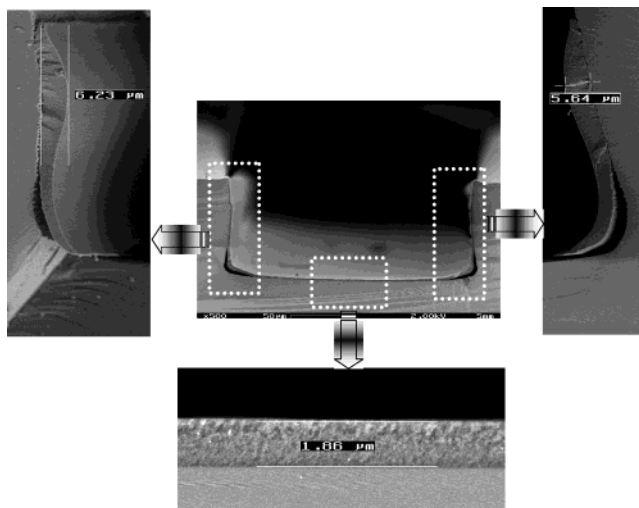


**Figure 8.** Cross section of a microchannel with detailed left and right sides and bottom of the microchannel with a thin film layer of Pt/ $Al_2O_3$  catalyst. (The researchers wish to express their gratitude to DARPA for funding Grant N66001-02-1-8942.)

a liquid precursor and then dry and calcine it to make a solid thin film adherent to the walls of the microchannel. Two basic methods were developed to infiltrate the microchannel with the liquid precursor:<sup>71,72</sup>

*Method I* was designed for an unbonded microreactor. A micropositioner-controlled pipet tip was used to inject the liquid into the channel from the open top of the channel.

*Method II* was designed for a bonded microreactor. After the channel was sealed with a Pyrex top plate using the anodic bonding technique, the liquid precursor was infiltrated into the microreactor through the outlet of the reactor under slight pressure and withdrawn. A thin film of solution remained on the walls of the microchannel.

The cross section of a microchannel with the catalyst film was investigated by scanning electron microscopy (SEM) (Figure 8).<sup>33,71,72</sup> As can be seen from the figure, the thickness of the film in the microchannel was not completely uniform. The thinnest film was on the bottom of the channel, and the thickness increased on the walls and bulged at the top. The thickness of the film catalyst infiltrated in the manner described above was in the range 1–8  $\mu m$ . The researchers reported that experience with other microchannel geometries showed the shape was connected to the microchannel dimensions, sol density, and capillary forces. The catalyst adhesion to the microreactor walls was satisfactory; however, the thin film can detach in the corners (Figure 8). More exploration must be conducted to optimize film adhesion for robustness.<sup>33,72</sup>

Microreactors with the thin film catalyst deposited as described were repetitively tested across a wide temperature range. The feed was composed of 1.7% CO, 68%  $H_2$ , and 21%  $CO_2$  with  $N_2$  as the balance. The flow rate was maintained at 5  $Ncm^3/min$  ( $\sim 0.6 W_e$ ) which the researchers believed would be enough for a 0.5  $W_e$  fuel cell. However, using the DOE assumptions (45% for reformer systems), this would translate into approximately 0.27  $W_e$ .<sup>79</sup> After each

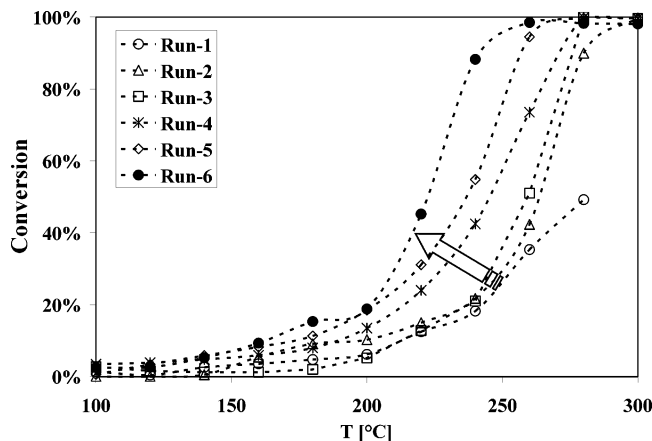


**Figure 9.** Catalyst activity increase as a function of aging: initial CO conversion with temperature increase for repeated runs [reformat 5 (N cm<sup>3</sup>)/min and dry air 0.5 (N cm<sup>3</sup>)/min,  $\lambda = 2.57$ ]. (The researchers wish to express their gratitude to DARPA for funding Grant N66001-02-1-8942.)

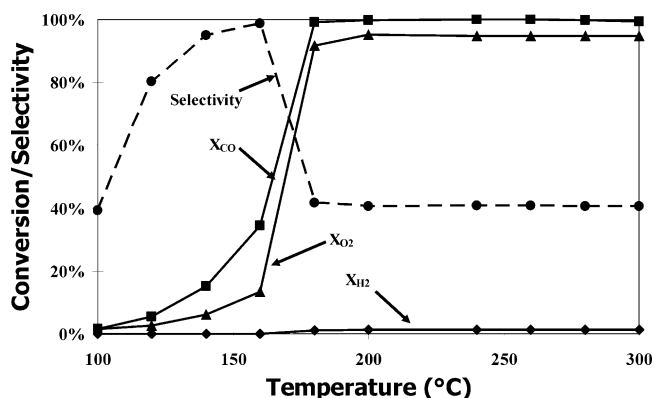


**Figure 10.** Conversion of CO, O<sub>2</sub>, H<sub>2</sub>, and CO<sub>2</sub> selectivity as a function of temperature [reformat 5 (N cm<sup>3</sup>)/min and dry air 0.5 (N cm<sup>3</sup>)/min,  $\lambda = 2.57$ , estimated catalyst weight = 1.5 mg].

run, the microreactor was reduced in pure hydrogen.<sup>73,75,77</sup> Figure 9 shows that the initial conversion was low until the ignition temperature was reached, where a steep increase in conversion was observed and approximately 100% conversion was achieved within about a 60 °C window. Characteristic behavior for CO, H<sub>2</sub>, and O<sub>2</sub> conversions and CO<sub>2</sub> selectivity is shown in Figure 10.<sup>77</sup> The researchers observed that (1) the selectivity consistently increased with an initial conversion increase and topped at approximately 90% at about 10% conversion and (2) the selectivity dropped to approximately 40% at about 100% conversion and 180 °C (Figure 10). Repeated cycles showed that the catalyst continued to improve with initial cycling, and several cycles were necessary to reach its full activity.<sup>73,75,77</sup>

The catalyst remained active and did not start to deactivate for about 50 h on stream without any regeneration. After that, the catalyst activity started to drop slowly but steadily.<sup>73</sup> The deactivation could be caused either by sintering of Pt nanoparticles or by coke deposited on the Pt atoms. If the catalyst deactivation was caused by coking, regeneration may reestablish catalyst activity. However, regeneration in air did not improve catalyst activity, which suggests that the cause of deactivation was not coke.

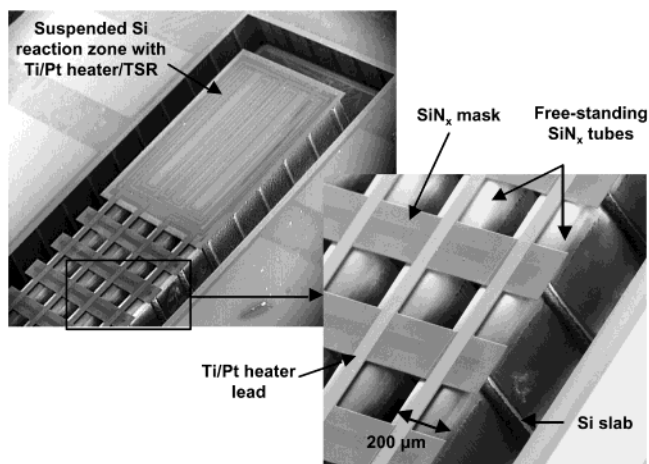


**Figure 11.** Suspended-tube reactor. (Reprinted with permission from ref 22. Copyright 2003 IEEE.)

More studies are needed to better understand catalyst deactivation and improve stability.

## 3.2. Power Supplies in the 1–10 W Range

### 3.2.1. MIT Suspended-Tube Reactor for 1–2 W Power Generation

Researchers at MIT developed an innovative suspended-tube microreactor (Figure 11) to produce up to 9 sccm of hydrogen (1.6 W) by thermally cracking ammonia.<sup>80</sup> A membrane for hydrogen purification and thermal electric generators was also integrated into the device.<sup>22,80,81</sup> Other important features of the system included a thin film heater, a temperature-sensing resistor, internal vertical posts within the channels, and passive stop valves. The reactor was designed for thermal isolation, which is considered essential, since “heat loss relative to heat generation is inversely proportional to characteristic length”.<sup>81</sup> The thermal isolation was obtained in two ways:<sup>22,80</sup> (1) low heat conduction, since the walls were 2 μm thick and 3 mm long and made of SiN, which has a low thermal conductivity, and (2) suspended-tube design, which allows for the vacuum packaging needed to reduce radiation losses at the high operating temperatures.

The reactor was fabricated using a silicon-based molding process. In this process, channels with internal vertical posts were formed initially by DRIE or potassium hydroxide wet etching techniques (Figure 12).<sup>22,80</sup> Once formed, an ultrathin silicon wafer is bonded to seal the channels. The next step is to coat the inside channel surfaces with low-stress nitrides by low-pressure vapor deposition. The silicon mold is then selectively removed by a process developed at MIT using fluorine gas, leaving the silicon nitride free-standing tubes. Thin film heaters and temperature-sensing resistors are fabricated on the surfaces of the tubes.

Packaging was designed to thermally isolate the device while maintaining electrical and fluid interconnects. The first step was to protect the device from mechanical shock by using spacer chips. Glass-frit bonding techniques were used to bond the chips to the reactor. Low-pressure vacuum packaging and

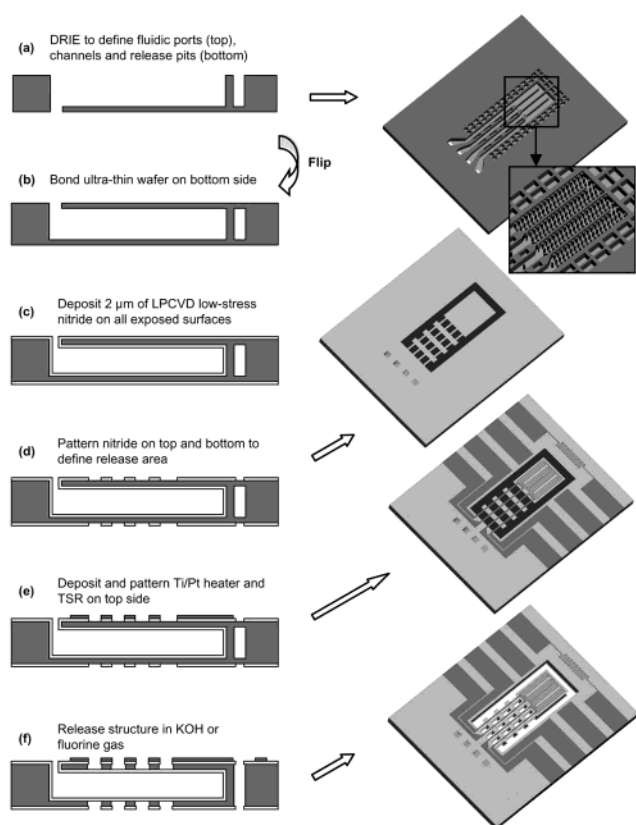


**Figure 12.** Suspended tube reactor fabrication process. (Reprinted with permission from ref 22. Copyright 2003 IEEE.)

infrared reflective coatings are planned in addition to these chips for further thermal isolation. These packaging strategies must allow for electric and fluidic interconnections. The electric interconnections are necessary for resistive heating for startup and operation when combustion is not used and also for temperature monitoring from temperature-sensitive resistors fabricated on the reactors.<sup>22,80</sup>

Noble metal catalysts were deposited into the tube reactors using a wash-coat technique.<sup>22,80</sup> An aqueous solid suspension containing  $\text{AlO}(\text{OH})$  and metal salt (e.g.,  $\text{IrCl}_4$  for iridium catalyst deposition) is wicked into the tubes. The combustion catalyst was required only in the reactor section of the tubes and not in the reactant feed tube to control where the combustion reaction occurred. Therefore, a cleverly designed passive stop valve was built at the junction between the combustor reactor and the inlet tube, which prevented the wash-coat solution from wicking into the inlet tube (Figure 13). After drying,  $\text{AlO}(\text{OH})$  was calcined to  $\text{Al}_2\text{O}_3$  by heating the reactor to 500 °C in nitrogen or air. Finally, the metal catalyst was made by reducing the metal salt in a hydrogen atmosphere at 300 °C for 1 h. Other catalyst materials and deposition techniques are under development.

Arana et al.<sup>22</sup> have performed extensive modeling and thermal characterization experiments on their reactor design. They modeled their design consisting of two suspended  $\text{SiN}_x$  tubes linked with slabs of silicon using two-dimensional computation fluid dynamics and a heat transfer model (Femlab, Comsol Inc.). The heat of reaction of the steam reforming or

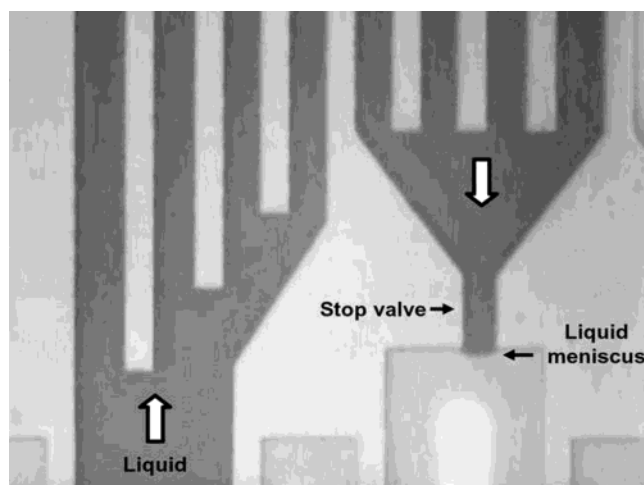


**Figure 13.** Suspended tube reactor stop valve. (Reprinted with permission from ref 22. Copyright 2003 IEEE.)

ammonia decomposition was not included. The model assumed incompressible fluid flow and close to ideal packaging (negligible losses through the conduction, convection, and radiation). The fluid flows for both the combustion and reforming streams were 10 sccm, and the pressure was atmospheric. The temperature map (Figure 14) shows that the silicon slabs were efficient at transferring thermal energy between the tubes. The model also shows a temperature gradient in the fluids themselves. This temperature gradient may change due to the heat of reaction in the actual system.

The reformer reactor performance as an ammonia cracker was evaluated. The experiments were conducted using a reformer feed composed of 6 sccm ammonia. The reactor was heated with the electric heaters to determine the heater power required to achieve high conversion. In these experiments, approximately 97% of the ammonia feed was converted to hydrogen at ~900 °C (approximately 1.8 W) when operating at atmospheric pressure.<sup>22,80</sup>

In other experiments, the combustor performance was examined. The combustor was operated with hydrogen or butane in air as the reactant. No reason was given for the selection of butane and not ammonia, which was used for the reformer testing, or methanol, which they also proposed to use. For startup, electrical heaters raised the reactor temperature to the ignition temperature in under 1 s, but once combustion was ignited, no further electrical heating was required. Approximately 1.6 W of thermal power was generated by combusting 0.8 sccm butane in a stoichiometric mixture of air, which should be sufficient power for the ammonia cracking reactions to occur.<sup>22,80</sup>

### 3.2.2. Lehigh University Methanol Reforming Reactor

Researchers at Lehigh University are developing a methanol reforming silicon reactor with a palladium membrane for a hydrogen purification system built using semiconductor fabrication techniques.<sup>82–84</sup> The device is designed to produce hydrogen for fuel cells for portable electronic devices, such as laptop computers and cell phones.

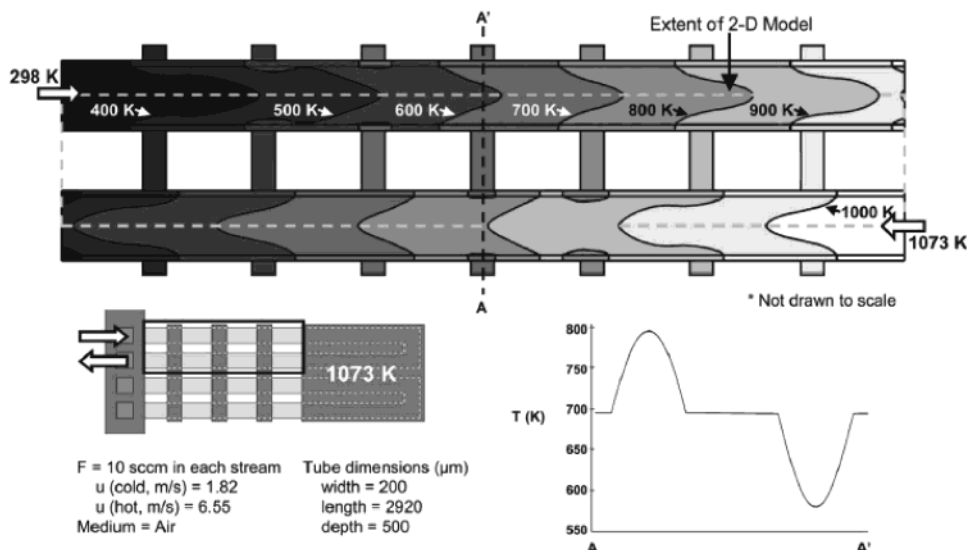


**Figure 14.** Temperature profile from a 2-D CFD simulation of the suspended-tube reactor (in a vacuum ambient assuming no radiation losses). (Reprinted with permission from ref 22. Copyright 2003 IEEE.)

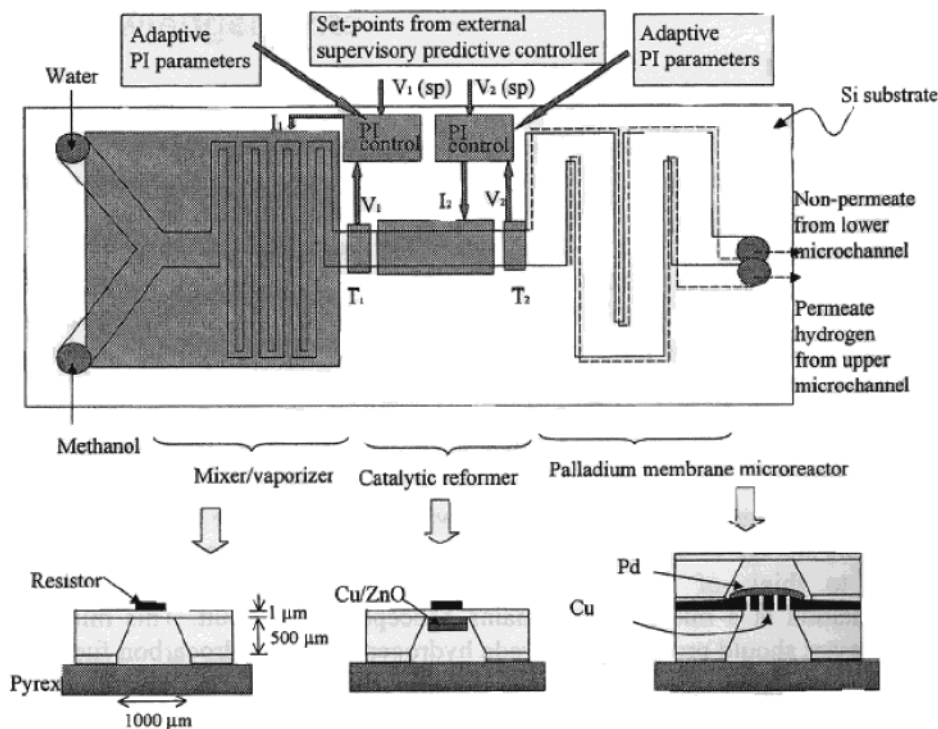


**Figure 15.** Microreformer illustration. (Reprinted with permission from ref 82. Copyright 2001 Springer.)

The steam reformer is a serpentine channel with a channel width of 1000  $\mu\text{m}$  and depth of 230  $\mu\text{m}$  (Figure 15). Four reformers were fabricated per single 100 mm silicon wafer polished on both sides. In the procedure employed to fabricate the reactors, plasma enhanced chemical vapor deposition (PECVD) was used to deposit silicon nitride, an etch stop for a silicon wet etch later in the process, on both sides of the wafer. Next, the desired pattern was transferred to the back of the wafer using photolithography, and the silicon nitride was plasma etched. Potassium hydroxide was then used to etch the exposed silicon to the desired depth. Copper, approximately 33 nm thick, which was used as the reforming catalyst, was then deposited by sputter deposition. The reactor inlet was made by etching a 1 mm<sup>2</sup> hole into the end

of one of the channels. First the reactor was covered by black wax, except the end where the hole was desired; then the wafer was etched using potassium hydroxide to form the hole, and the black wax was removed.<sup>82</sup> The wafer was diced to make four separate reformer reactors.

The reformers were tested in a custom-made stainless steel housing unit.<sup>82</sup> Graphite pads with appropriate holes for reactant and product interfaces were used as gaskets in the housing. The goal of the tests was to determine if hydrogen could be produced using this configuration. A methanol and water (50:50 by weight) mix was externally vaporized and fed to the reactor, which was maintained at 250 °C. The feed rate was 0.142 g/min. The researchers reported that 0.092 mol of hydrogen per mole of methanol fed

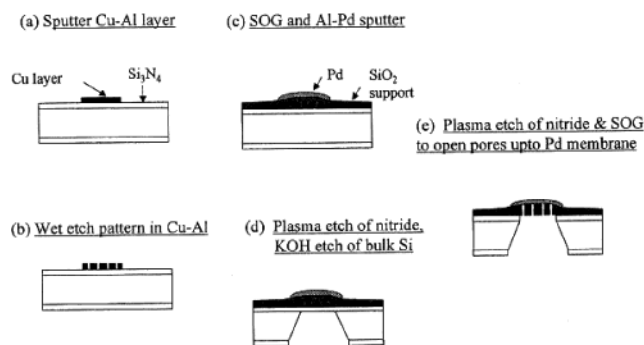


**Figure 16.** Microscale palladium membrane. (Reprinted with permission from refs 83 and 84. Copyright 2001 and 2002 Springer.)

to the reformer was produced, about 3% of the theoretical maximum of 3 mol of hydrogen per mole of methanol. The next step in the reformer development will be to incorporate a Cu/ZnO catalyst into the reactor.<sup>82</sup>

The palladium-based membranes were a composite of four layers: copper, aluminum, spin-on-glass (SOG), and palladium. The copper, aluminum, and SOG layers served as a structural support for the thin palladium layer, and the copper was also intended for use as a WGS catalyst in the reactor to increase the yield of hydrogen.<sup>83,84</sup> The membrane was fabricated in five steps on a 100 mm silicon wafer polished on both sides and with silicon nitride deposited on both sides (Figure 16).<sup>83,84</sup> First, 66 nm of copper followed by 200 nm of aluminum were sputter deposited on the front of the wafer. The copper was to be used as the catalyst for the WGS reaction, and the aluminum was added to increase the mechanical strength of the free-standing membrane. These metal layers were wet etched into the desired pattern. Next, 500 nm of SOG was deposited and cured for 30 min at 250 °C. The SOG planarized the wafer. A thin layer of aluminum, for adhesion promotion, followed by 200 nm of palladium, was then sputter deposited onto the SOG. The backside of the wafer was patterned by plasma etching the silicon nitride and using a potassium hydroxide solution to etch the bulk silicon, making the reactant flow channels. Pores with a 5.5 μm diameter were opened up to the palladium membrane by plasma etching the silicon nitride and SOG. Two pore arrangements were used: one with pores 14 mm apart and the other with pores 20 mm apart.<sup>83,84</sup>

Using similar housing as described for the reformer reactor, the membrane's mechanical strength and static hydrogen permeation tests were performed at room temperature. The mechanical strength was tested using pure nitrogen gas. Pressure differentials greater than 15 psi were achieved before the membrane failed.<sup>84</sup> For the hydrogen permeation tests, one side of the membrane was pressurized to 2 psi with a nitrogen hydrogen mixture (80% nitrogen). At this low temperature and pressure, hydrogen was detected on the other side of the membrane using a quadrupole ion-trap mass spectrometer.<sup>84</sup> Typical palladium membranes are 25 μm thick or more and are operated at elevated temperatures, >100 °C (usually closer to 300 °C), and elevated pressures,

**Table 3. Vaporizer and Reformer Operating Conditions and Performance (Adapted from ref 88)**

vaporizer temperature	120 °C
reformer temperature	260 °C
pressure	1 atm
steam-to-carbon molar ratio	1.1:1
reactant flow rate	12 cm <sup>3</sup> /h
conversion	>90%
product gas composition	73.4% hydrogen 25% CO <sub>2</sub> 1.6% CO
hydrogen production rate	0.498 mol/h = 186 sccm
estimated electric power <sup>a</sup>	15 W

<sup>a</sup> Assuming 60% efficient fuel cell utilizing 80% of the hydrogen.

typically >100 psi, and have hydrogen permeation rates such as 1 cm<sup>3</sup> H<sub>2</sub> (STP)/(cm<sup>2</sup> min) (see, for example, refs 85–87). The Lehigh University researchers will need to be able to achieve similar permeation rates.

### 3.3. Reactors in the 15–100 W Range

#### 3.3.1. Korea Institute of Energy Research 15 W Power Generation

Park et al., who are developing a methanol fuel processor, so far have tested designs for the vaporizer and methanol reformer using electric heating cartridges to provide the thermal energy for the endothermic reaction (Table 3).<sup>88</sup> A sheet architecture was used to build the units. The microchannels for both the vaporizer and reformer were 500 μm wide and 33 mm long and were patterned onto metal sheets (200 μm thick) using wet chemical etching techniques. Three sheets were stacked to make the total channel depth 600 μm. In addition, manifold sheets with two holes for a flow path and triangular manifolds to enable a more uniform flow distribution were placed on the top and bottom of the stack. The dimensions of the reformer and vaporizer were 70 × 40 × 30 mm<sup>3</sup> (excluding fittings).

The catalyst bed was a coated wall reactor using commercial CuZnAl catalyst. An alumina sol was used to enhance the adhesion of the catalyst to the channel walls. After the shims were washed thoroughly, the alumina adhesion layer was deposited using an alumina sol (NYACOL AL20DW colloidal alumina, PQ Corporation) and then dried at 60 °C. To decrease the surface tension of the wash-coat solvent, small amounts of 2-propanol were added to a catalyst slurry of ICI Syntex 33–5 catalyst, with 20 wt % alumina sol and water. The catalyst was calcined at 350–400 °C for 2 h after air-drying. Before testing, the catalyst was reduced by flowing H<sub>2</sub>/N<sub>2</sub> over it at 280 °C.

The reactor was tested using a range of methanol and water concentrations, and researchers found the best results using a water and methanol mixture with a steam-to-carbon ratio (S:C) of 1.1:1.<sup>88</sup> They were able to achieve 90% conversion at 260 °C with a reactant liquid flow rate of 12 cm<sup>3</sup>/h. Assuming a fuel cell efficiency of 60% and 80% hydrogen utilization, they estimated the output power to be 15 W. Eventually the complete system will include a cata-

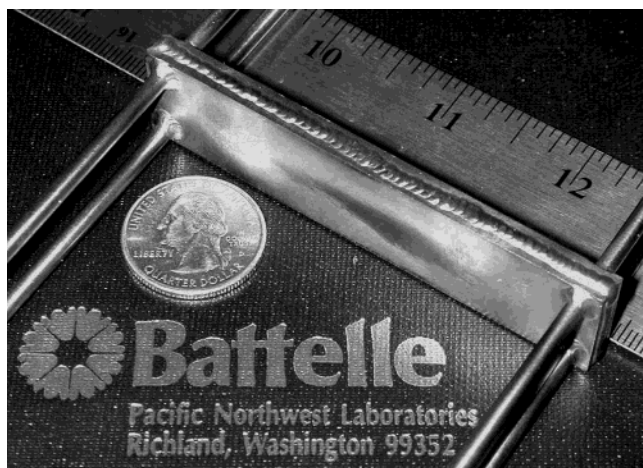


**Figure 17.** 25–50 W integrated fuel processor.<sup>64</sup>

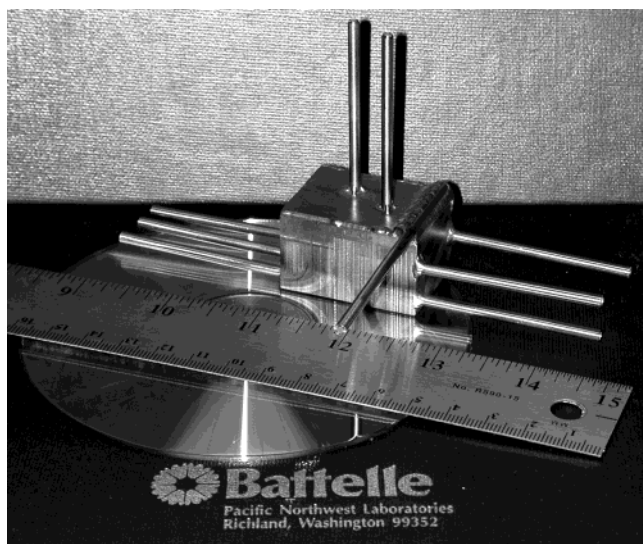


**Figure 18.** 50 and 100 W integrated fuel processor-cube design.<sup>89</sup>

lytic combustor and carbon monoxide cleanup units.<sup>88</sup> They will also need to achieve >99% methanol conversion or develop a way to deal with the unconverted methanol.

### 3.3.2. Battelle, Pacific Northwest Division, 15–100 W Power Generation

Fuel processors being developed at Battelle provide 15 W to over 100 W equivalents of hydrogen from methanol fuel.<sup>64,89–91</sup> Two architectures based on microchannel technology<sup>14,15</sup> were used in this work (Figures 17 and 18), which enabled a scalable fabrication over this wide range. The processors consisted of fuel vaporizers and preheaters for both the combustion reactants and steam reforming reactants, a combustor, a steam reformer, heat exchangers, and recuperators.<sup>64,89–91</sup> The reactors were assembled using a combination of welding, brazing, and diffusion bonding techniques, although the specifics of the techniques and the laminate layer designs are not reported.

In addition to the microchannel technology, Battelle has developed a stable, nonpyrophoric, carbon dioxide selective, methanol reforming catalyst.<sup>31,32,89–91</sup> The catalyst has been demonstrated to be stable in

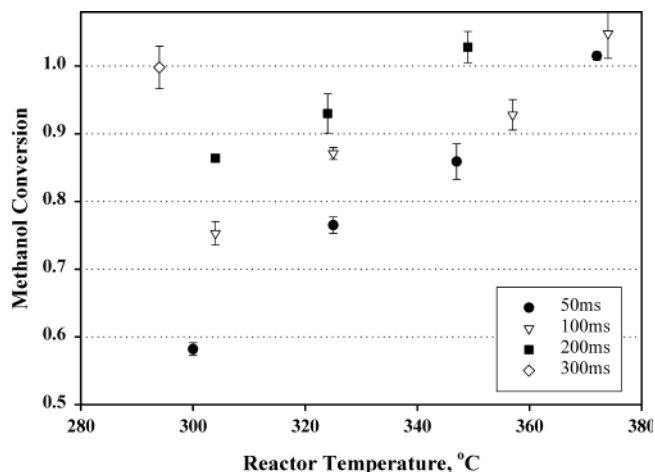


**Figure 19.** Battelle's methanol specific reforming catalyst. Reactor conditions: atmospheric pressure, reactant feed 50:50 by weight methanol and water mixture, 24 000–50 000 h<sup>-1</sup> GHSV. The conversion was reported as moles methanol reacted/moles methanol fed. (Reprinted with permission from ref 91. Copyright 2002 Elsevier.)

**Table 4. Battelle Fuel Processor Performance<sup>70</sup>**

device design point	20 W	50 W	100 W
demonstrated power, W	6–34	26–54	60–170
volume, cm <sup>3</sup>	<20	<25	<30
mass, g	<150	<175	<200
power density, W/L	1800	2100	5600
thermal efficiency, %LHV	28–63	62–84	>80%
energy density, <sup>a</sup> Wh/kg	520–1500 <sup>b</sup>	1032–1732 <sup>c</sup>	1600–2150 <sup>d</sup>

<sup>a</sup> Assumes 80% of hydrogen is reacted in the fuel cell, and the fuel cell is 60% efficient. <sup>b</sup> Assumes 1 kg device hardware, 14 day mission, water recycle, anode gas recycle, and parasitic power = 3 W. <sup>c</sup> Assumes 3 kg device hardware, 14 day mission, water recycle, anode gas recycle, and parasitic power = 5 W. <sup>d</sup> Assumes 5 kg device hardware, 14 day mission, water recycle, anode gas recycle, and parasitic power = 10 W.

air, even at elevated temperatures (~200 °C), without loss of activity or carbon dioxide selectivity.<sup>89–91</sup> No deactivation was observed in a 1000 h lifetime test operating with a water and methanol mixture and at a gas hourly space velocity (GHSV) of 36 000 h<sup>-1</sup>.<sup>89–91</sup> The water-to-methanol molar ratio for the mixtures ranged from 3.0:1 to 1.2:1 without any reported difference in lifetime or carbon dioxide selectivity. Typical performance is shown in Figure 19. This catalyst was engineered for operation in low-pressure-drop microchannel reactor configurations.

Recent fuel processor performance is summarized in Table 4. The fuel processors were operated at atmospheric pressure, and the water and methanol feed mixture was about 60 wt % methanol. The typical composition of the reformat stream was 72–74% hydrogen, 24–26% carbon dioxide, and 0.5–1.5% carbon monoxide on a dry gas basis. The carbon monoxide levels were significantly below equilibrium (5.4% at 350 °C), but they still require additional cleanup for use in fuel cells.<sup>89–91</sup> The fuel processor efficiency was calculated using eq 5 and was reported to be greater than 80%. It is interesting to note that increasing the power 5-fold, from 20 to 100 W, only resulted in a 50% increase in volume and a 33% increase in mass.

Researchers recently began incorporating a catalytic carbon monoxide cleanup system based on

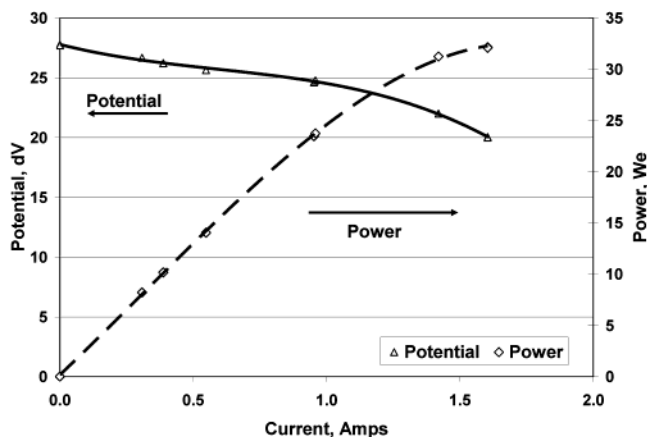


**Figure 20.** Fuel cell performance demonstration for the Battelle methanol processor and the carbon monoxide removal reactor.<sup>89</sup>

selective carbon monoxide methanation, which decreased the CO to below 100 ppm.<sup>70</sup> The low carbon monoxide stream from the methanol processor and carbon monoxide removal reactor were used to operate an H-Power fuel cell (Figure 20).<sup>89</sup>

Current efforts are focusing on optimizing the carbon monoxide removal reactor and developing a system prototype using commercially available pumps, blowers, fuel cells, valves, and controllers.<sup>70</sup> In addition, durability testing along with thermal cycling needs to be done.

### 3.3.3. MiRTH-e 20–100 W Reactor

The European Union is funding a project to develop microreactor technology for hydrogen and electricity (MiRTH-e) in the 20–100 W size range using methanol steam reforming.<sup>92,93</sup> Participants include researchers from Shell Global Solutions International (The Netherlands and Great Britain), the Institut für Mikrotechnik Mainz (IMM, Germany), the MESA Research Institute (The Netherlands), the ECN Energy Research Foundation (The Netherlands), The Laboratory of Chemical Reactor Engineering at Eindhoven University of Technology (The Netherlands), and the Laboratoire des Sciences du Génie Chimique of CNRS (France).<sup>92</sup>

Initially, the reactor was to be built using silicon wafers,<sup>92</sup> but more recent efforts have focused on a stainless steel reactor.<sup>93</sup> The reformer,  $7.5 \times 4.5 \times 11.0$  cm<sup>3</sup> (371 cm<sup>3</sup>), houses up to 15 stainless steel plates (0.5 mm thick) with chemically etched microchannels and heating cartridges. Conventional and laser micromachining techniques were used to fabricate the reformer body. The microchannel dimensions are  $0.05 \times 0.035 \times 5.0$  cm<sup>3</sup>. The reactor inlet was carefully designed to allow uniform flow conditions.<sup>93</sup>

To process the methanol and water mix, a CuZnAl catalyst was wash-coated onto the microchannel walls. The alumina was deposited by dipping the plates into a 20% alumina suspension, which also included a stabilizer and a binder. After any excess was wiped off, the plates were calcined at 600 °C for 1 h in air. Air was removed from the pores by placing the calcined plate in a vacuum. The alumina wash-

coat had a specific area of 72 m<sup>2</sup>/g, a pore diameter distribution with a maximum of 45 nm, and an average thickness of 10 μm. The copper zinc oxide catalyst (3:1 Cu/Zn ratio) was deposited onto the alumina by impregnating the alumina with a copper zinc nitrate solution and calcining at 300 °C. A loading of 8 wt % was obtained following this preparation technique, although higher loading can be obtained by repeating the impregnation process.<sup>93</sup> However, increasing the loading this way may fill in pores, resulting in a net loss of surface area and accessible active catalyst sites hurting performance, so an optimum loading will need to be found.

The reactor performance was evaluated using five wash-coated plates with microchannels. The catalyst was reduced in an atmosphere of 5% hydrogen in nitrogen at 240 °C. Before operation, the catalyst was pretreated at 250 °C for 2 h with a mixture of 30% nitrogen, 47% water, and 23% methanol. This pretreatment brought the catalyst to stable activity before measurements were completed.<sup>93</sup> A vaporized mixture of water and methanol (2:1 molar ratio) was fed to the reactor at flow rates from 500 mL/min (STP), and the reactor was operated at atmospheric pressure and 280 °C. Higher-temperature operation was not possible due to limitations of the reactor design. Under these conditions, methanol conversion of 65% was achieved, which translates into approximately 30 W, assuming a fuel cell efficiency of 64%.<sup>93</sup> Therefore, increasing the plate number to the 15-plate maximum would result in approximately 90 W.<sup>93</sup> Improvements in performance are expected to be achieved by increasing the catalyst loading to 16 wt %. The researchers also reported the need for developing a selective oxidation reactor to decrease the carbon monoxide levels to below 20 ppm.

### 3.3.4. Motorola Methanol Fuel Processor

A research team from Motorola is developing a methanol fuel processor for use in portable applications. The fuel processor is constructed using ceramic fabrication techniques and includes a fuel vaporizer, a steam reformer, and a catalytic combustor.<sup>94</sup> The vaporizer is a small chamber loaded with a high-surface-area felt, which allows the high heat transfer rates essential for methanol and water vaporization.<sup>94</sup> A packed-bed design with alumina-supported CuO/ZnO powder catalyst was selected for the reformer, with the combustor designed to react excess hydrogen from the fuel cell and methanol with air using a platinum catalyst. The catalyst was wash-coated onto the combustor walls.<sup>94</sup> High methanol conversion rates were achieved at low temperatures (230 °C) using this design. An interesting feature of this development project was the use of PBI-doped with phosphoric acid based fuel cell technology similar to that developed by Case Western Reserve University.<sup>94</sup> As with the microscale fuel cell using PBI technology described previously, the Motorola fuel cell could operate at high temperatures, enabling the fuel cell to tolerate high levels of carbon monoxide. This CO tolerance negated the need for additional reformat cleanup.<sup>94</sup>

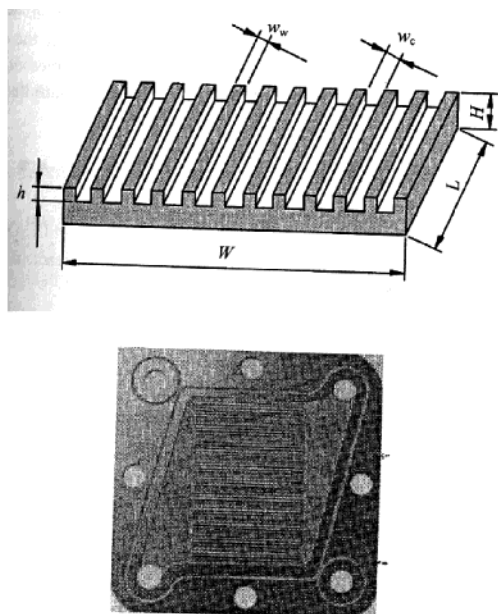


**Figure 21.** Microchannel reactor chip. (Reprinted with permission from ref 34. Copyright 2003 Elsevier.)

### 3.3.5. MesoSystems Technology in the 50–100 W Range

MesoSystems is developing a 50 W portable power supply using ammonia as the fuel.<sup>95,96</sup> The system consists of an ammonia cracking reactor, an ammonia adsorbent, a membrane, heat exchangers, and power controls. They have integrated the system with the necessary pumps, fans, and controls and tested it with fuel cells.

The ammonia cracking reactor is based on what they call mesochannel reactors of stainless steel construction. The reactor operates between 575 and 625 °C at 1 or 4 atm pressure depending on if a membrane is used. Specifics about their membrane and catalysts were not reported. There was an ammonia bypass of 0.2–0.5 wt % of the ammonia feed. Even this small amount of ammonia will irreversibly damage the fuel cell, so they include a proprietary adsorbent. The adsorbent has a capacity of up to 10 wt % ammonia at ppm-level feed stream conditions. Thermal management for the reactor system was accomplished by using compact heat exchangers and innovative high-temperature vacuum insulation panels. The system targets include a 5 min startup and 1000 W h electric power in a 1 L (1 kg) package. This translates into a ~6 wt % hydrogen storage density. They report to have demonstrated this system with H Power Corporation's SSG-50 fuel cell; however, no data were available.<sup>95</sup> In addition, no lifetime or other durability data were reported.

## 3.4. Reactors $\leq$ 500 W

### 3.4.1. Scalable Methanol Autothermal Reforming Reactor

Researchers at the Chinese Academy of Sciences are developing a scalable methanol autothermal reforming (ATR) reactor.<sup>34</sup> The microchannel reactor will be composed of multiple "reactor chips" (Figure 21), with each chip able to process enough methanol for approximately 100 W<sub>e</sub> hydrogen. Both aluminum and stainless steel were evaluated for use as the chip

substrate. The chips were approximately 7.5 × 7.5 cm<sup>2</sup>. The channels were chemically etched into the metal substrates. The stainless steel chip was 0.34 mm thick and had 48 channels, each channel being 0.17 mm deep, 0.5 mm wide, and 30 mm long. The aluminum chip was 0.8 mm thick and had 38 etched channels, each channel being 0.4 mm deep, 0.8 mm wide, and 30 mm long. The chips were tested in a metal housing that allowed the temperature to be controlled and provided access for the reactant and product streams.

A CeO<sub>2</sub>–ZrO<sub>2</sub> supported platinum catalyst was used in this reactor.<sup>34</sup> The chips were prepared for the catalyst deposition using the following method. First, the surfaces were cleaned with a Na<sub>2</sub>SiO<sub>3</sub> solution to remove any oil and other residues. After the reactor chips were washed with distilled water and dried, CeO<sub>2</sub>–ZrO<sub>2</sub> was deposited onto their surfaces, using wash coating techniques. These reactor chips were then dipped into a solution of Pt(NH<sub>3</sub>)<sub>4</sub>·(OH)<sub>2</sub> (0.1 g/mL) and dried at 120 °C, followed by calcinations at 400 °C in air for 3 h. Before being used, the catalyst was reduced in a 10% hydrogen in nitrogen atmosphere at 400 °C for 2 h.<sup>34</sup>

After the catalyst was reduced, the microreactor was tested. A water and methanol mixture (1.2:1) was used as the fuel, and the oxygen-to-methanol molar ratio was 0.3:1.<sup>34</sup> The oxygen was supplied from air. Using the stainless steel reactor chip with a feed of 186 000 h<sup>-1</sup> gas hourly space velocity (GHSV), greater than 99% of the methanol was reacted (reactor conditions = 450 °C and atmospheric pressure). The product gas dry flow was 820 L/h, with 43% being hydrogen (360 L/h). The composition was 43% hydrogen, 0.5% methane, and >15% carbon monoxide, with the rest being nitrogen (from the air feed for ATR operation) and carbon dioxide. The high carbon monoxide levels will require that WGS reactors and preferential oxidation (PrOx) reactors be developed to reduce the carbon monoxide to below 10 ppm.<sup>34</sup>

### 3.4.2. Portable Power Using a Propane Cracking Reactor System

Ledjeff-Hey et al. are developing a hydrogen generator able to provide approximately 160 W<sub>e</sub> of hydrogen by cracking propane.<sup>97,98</sup> The overall system consists of two propane cracking batch reactors, a methanation reactor, a combustor, air blowers, eight magnetic valves, a control unit, a fuel cell, an accumulator, and a charge controller (Figure 22). In this system, propane is cracked, producing hydrogen and coke in one reactor while the other is being regenerated.<sup>98</sup> Initially, some carbon monoxide and carbon dioxide are produced as the residual air from catalyst regeneration is being depleted. The carbon monoxide is removed by the simple methanation reactor in the system. Because the regeneration cycle requires approximately 15 min, the reactor operation is switched every 15 min from cracking to regeneration. During regeneration, coke formed on the catalyst is burned off using air. A key advantage of the propane cracking system is that the product gas has a high hydrogen concentration (>90%) and low

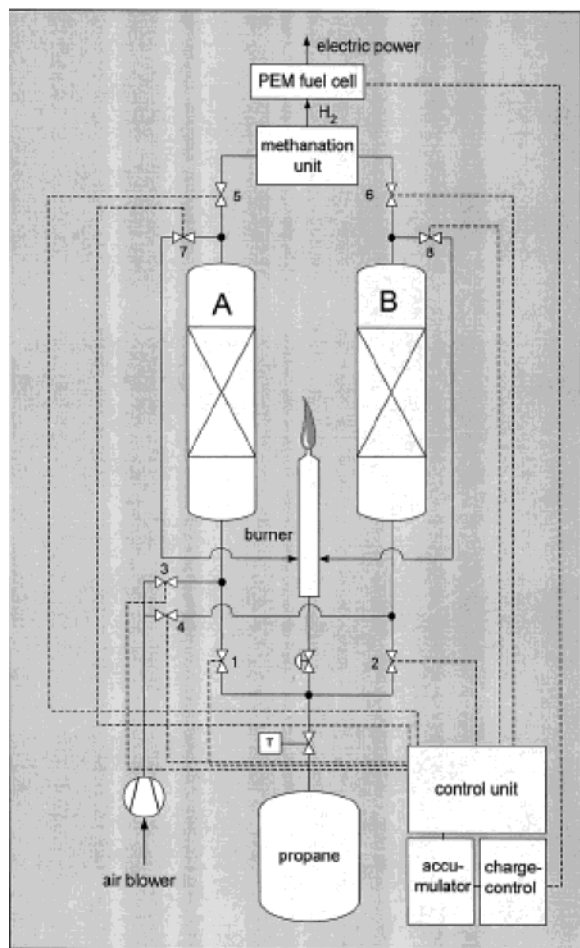


**Figure 22.** Schematic of a portable fuel cell system with a propane cracker. (Reprinted with permission from ref 98. Copyright 2000 Elsevier.)

carbon monoxide concentration (<1% after the initial 2 min of operation)<sup>98</sup> However, the authors did not mention the possibility of fouling due to carbon formation. A study on the long-term durability of the system will be interesting.

The catalyst used in this process was a proprietary precious metal catalyst on alumina that was stabilized with a rare earth metal (to prevent sintering).<sup>98</sup>

The researchers reported that this catalyst did not deactivate as quickly as commercially available precious metal catalysts tested.

The complete system with fuel cell is under development. Its projected cost will be \$400–500 (U.S. dollars) for a 130  $W_e$  output.<sup>98</sup> The system efficiency is estimated to be 9%. This efficiency includes parasitic losses and an assumed fuel cell efficiency of 50%. The parasitic power requirements by the BOP components are about 70  $W_e$ , mostly from the eight magnetic valves, which is one cause for the low system efficiency.<sup>98</sup> The researchers are looking for lower-power magnetic valves and other solutions to decrease the parasitic power requirements.<sup>98</sup>

### 3.4.3. Methanol Reforming Reactors for a 200 $W_e$ Fuel Cell Power System

Pfiefer et al. are developing a methanol fuel processor system using steam reforming for a 200  $W_e$  fuel cell based power supply.<sup>99,100</sup> The researchers are currently working on the methanol reformer reactors, heat exchangers, combustors, and preferential oxidation reactors (Figure 23) for the system.<sup>100</sup> The reactor bodies are either stainless steel or copper.

For the chemical reactor, the researchers used a nanoparticle catalyst deposited on metallic microstructured foils.<sup>99</sup> They tested Cu/ZnO and Pd/ZnO catalysts deposited on the microstructured foils. The Cu/ZnO catalyst was more active than the Pd/ZnO catalyst and had a lower selectivity to undesired carbon monoxide.<sup>100</sup> However, because the Pd/ZnO catalyst was more stable, it was selected for use in their fuel processor.<sup>100</sup> The Pd/ZnO carbon monoxide selectivity of the powder catalyst pressed into a pellet was lower than that of the nanoparticle catalyst deposited on the microstructured foils. This effect was attributed to contact phases between the catalyst and the metal foils.<sup>100</sup>

The reformers were operated at 1.25 bar and up to 310 °C. The feed was composed of 75 g/h of water and 70 g/h of methanol (1.9:1 S/C molar ratio). At 310 °C, over 80% methanol conversion was achieved, with a low amount of carbon monoxide present (<1%). This results in approximately 160 W electric-

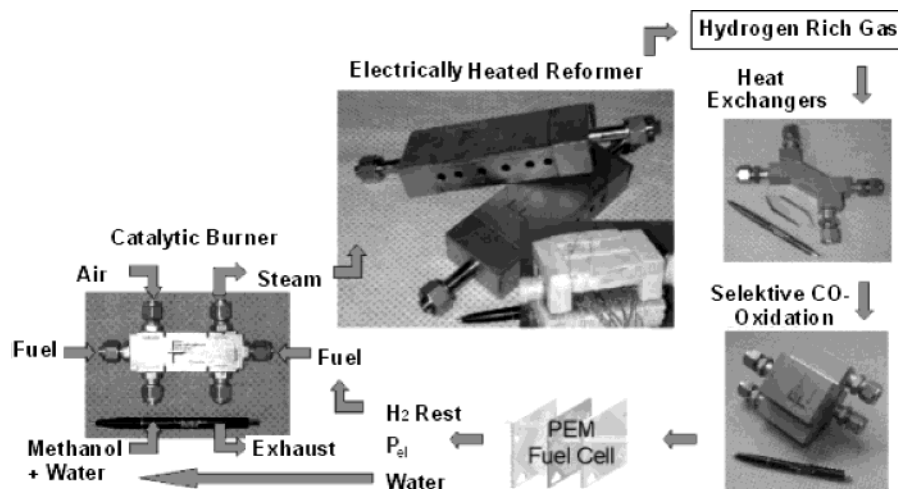


**Figure 23.** Methanol–steam reformers, heat exchangers, combustor, and selective oxidation reactors; the body material was stainless steel.<sup>100</sup>

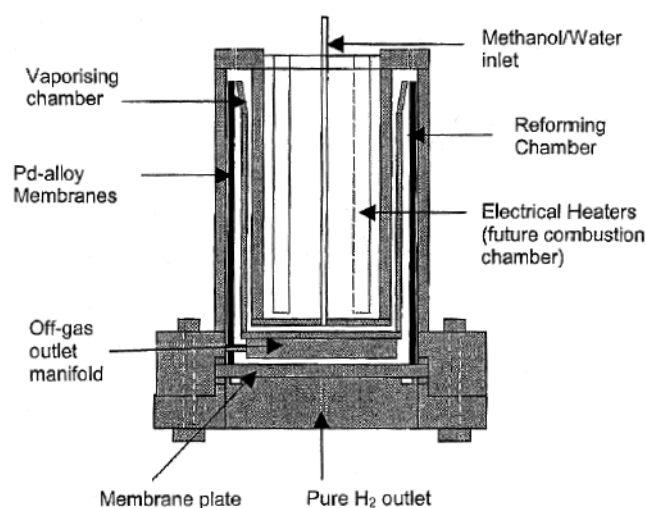


**Figure 24.** Schematic diagram of the compact steam-methanol processor.<sup>102</sup>

ity production from a 40–45% efficient fuel cell. Therefore, at 100% methanol conversion, the power would be approximately 200 W.<sup>100</sup>

#### 3.4.4. Royal Military College of Canada 200–300 W System

Researchers at the Royal Military College of Canada are developing fuel cell hydrogen generation based on methanol reforming technology.<sup>101–103</sup> They have developed empirical correlations for methanol reforming at 1–4 atm and carbon monoxide yields.<sup>103</sup> Numerical models for conventional packed-bed methanol reforming reactors have been developed.<sup>101</sup> The models included radial heat and mass distributions and also examined deactivation of the Cu/ZnO/Al<sub>2</sub>O<sub>3</sub> catalyst in the reactor.<sup>101</sup> In addition, the researchers are working on a miniature methanol reformer that will use a membrane for hydrogen purification in the final device.<sup>102</sup>

The fuel processor is sized to provide enough hydrogen for a 200–300 W fuel cell while being the size of a “generous coffee cup”.<sup>102</sup> A measured volume and mass was not reported. It uses a concentric annular design, which will eventually incorporate a combustion chamber (currently electrical heaters) in the middle of the annulus, with a vaporizer, reforming chamber, and palladium alloy hydrogen purifier forming layers (Figure 24). Incorporating a palladium membrane enables pure (>99.999%) hydrogen to be produced but requires elevated pressure operation (>70 psi).<sup>102</sup> The fuel processor contains 259 g of copper-based Sud Chemie G66b methanol steam reforming catalyst (bulk density = 1.4 g/cm<sup>3</sup>). The reformer and vaporizer components of the device

have been tested using electric heating, and other unit operations will be incorporated in the future.<sup>102</sup>

The reformer was operated for over 554 h, which included 402 h of reforming operation and 152 h of “hot standby.” During hot standby, the catalyst was maintained in the reduced state by flowing 50 cm<sup>3</sup> of hydrogen through the catalyst bed, which was kept at a minimum of 260 °C. The reactor was operated over a heater temperature range of 260–300 °C and up to 70 psia. A methanol and water mixture (S/C 1:1 molar) was fed at 1.5–3.5 mL/min. Table 5 summarizes the device performance.<sup>102</sup>

The next step in the processor development will be to integrate the palladium alloy membrane with the methanol steam reformer reactor. The researchers anticipate that the addition of the palladium membrane will improve the reactor performance due to in-situ hydrogen removal.<sup>102</sup>

#### 3.4.5. Emission-Free Reformer Concept for Portable Power Applications

Muradov<sup>60</sup> proposed using thermal decomposition of hydrocarbons to provide hydrogen for small fuel cells. If the environment is water- and air-free, then the hydrocarbon decomposition products will be coke and hydrogen. Collecting the carbon in a trap and physically removing it is proposed, rather than burning it, as others have done.<sup>60,98</sup> By collecting the carbon, the process reduces, and may even eliminate, CO and CO<sub>2</sub> emissions.<sup>60</sup> However, the authors did not address if carbon formed in this system will over time foul the reactor or how this type of system would be made feasible for a portable power supply. The fuel cell and pyrolysis system would consist of a catalytic pyrolytic fuel reformer with a carbon trap and catalytic combustor, a fuel tank, a sulfur trap, a methanator (to remove any residual CO or CO<sub>2</sub>), and a fuel cell. Heat for the pyrolysis reactions would be provided by burning the fuel cell anode off-gas. The pyrolytic reforming reactor concept has been demonstrated.

The pyrolytic reforming reactor was a packed bed in a quartz tube reactor. Quartz was selected to reduce the effect of the reactor construction material on the hydrocarbon decomposition rate.<sup>60</sup> The reactor was packed with 5.0 ± 0.1 g of AC (Darco KB-B) or CB (BP2000) carbon-based catalyst. The reactor was heated electrically and operated at 850–950 °C, and the reactants had a residence time of 20–50 s, depending on the fuel. The reactor was tested with propane, natural gas, and gasoline as the fuels. Experiments showed that a flow of 80% hydrogen, with the remainder being methane, was produced for over 180 min of continuous operation.<sup>60</sup> The carbon produced was fine particles that could be blown out

**Table 5. Methanol Steam Reforming Reactor Performance<sup>a</sup>**

burner/inlet <i>T</i> (°C)	methanol conversion (%)	methanol/water feed (mL/min)	gas composition, H <sub>2</sub> /CO/CO <sub>2</sub>	electrical equivalent (W <sub>e</sub> )
300/260	97.0	3.5	74.0/2.7/23.3	350
280/240	97.5	2.5	74.0/2.3/23.7	250
260/230	96.0	1.5	74.1/1.8/24.1	150

<sup>a</sup> Assumes 12 SLPM hydrogen = 1 kW<sub>e</sub>. Adapted from ref 102.

of the reactor into an acceptable container using nitrogen. The estimated energy density, based on the thermal heating value of the hydrogen produced for the reactor system (including tanks), was 1 (kW<sub>th</sub> h)/kg.<sup>60</sup> The researchers do not comment on the feasibility of using nitrogen to blow out the fine particles in a real world application. It would be interesting to note if they could use air rather than nitrogen so an additional storage tank is not needed. Nor have they reported lifetime and other durability issues for this system.

#### 4. Summary and Outlook

The development of microreactor technology to produce hydrogen for small, portable, fuel cell based power supplies is progressing at a rapid rate. These small reactors are being designed to provide hydrogen for subwatt power to hundreds of watts of power. Conventional wisdom dictates that, for a fuel cell power system, 1/3 of the volume is for the fuel cell, 1/3 is for the reformer, and 1/3 is for the balance of the plant. With the developments in microreactors reviewed here, the size of the reforming unit is shrinking considerably. Innovative fabrication techniques are being developed and used to manufacture these systems.

The technical success of these palm-sized reactors shows that microfabrication can be used to miniaturize unit operations that traditionally operate at a large scale. Methanol is the dominant fuel in the portable power ranges, but at the higher power levels (>200 W), higher hydrocarbon fuels, such as ethanol and gasoline, are being developed. Commercially available natural gas, propane, gasoline, diesel, or JP8 (for military applications) have not been used as fuels of choice because of their high sulfur content and other impurities. Although ammonia has many attractive characteristics, it has not received the same attention as hydrocarbon fuels.

For these microreactor systems to become viable, several significant technical areas need to be developed: processing system integration, sulfur removal, BOP integration, system durability, and fuel cell integration. The vast majority of microreactors reviewed were composed of the fuel reformer and lacked the other unit operations required for a complete fuel processor system. These additional unit operations include recuperative heat exchangers, vaporizers, a heat source (probably a catalytic combustor or electric heater), secondary conversion reactors (typically a two-stage WGS reactor system), and a final carbon monoxide removal or reduction system (typically a two-stage PrOx or a selective methanation system). Since only parts of the system were developed, efficiencies were often not reported. When efficiencies were reported, they were estimates based on assumed efficiencies of the other components. Although the membrane reactors eliminate the need for the secondary conversion reactors and a final carbon monoxide removal or reduction system, the other unit operations are still required. These unit operations need to be developed and thermally integrated with the fuel reformer. The durability and performance of the individual components and the

complete system will need to be evaluated and proved for a commercially viable product. There have been few lifetime tests, real world tests, or other durability tests done on the microreactors. This should be an area of further work.

For low-power (production of hydrogen for several watts or less power output) reactors, thermal losses caused low efficiencies. Although the reactor size was significantly reduced, in most cases, the piping connecting the reactor to instruments and other components could not be reduced by the same amount. Therefore, the tubing was relatively large and caused a relatively significant heat loss by conduction. In some cases, the thermal losses were reduced by decreasing the connector pipe size, by using advanced insulation, or by using vacuum packaging. The researchers need to continue incorporating these techniques and technologies to improve the system efficiencies, in addition to developing new and innovative ways to prevent heat loss or recapture heat.

Methanol was the fuel of choice for many of the smaller systems due to its low processing temperature and low contaminant (sulfur) level. However, the high energy density of more readily available hydrocarbons, such as propane, natural gas, gasoline, diesel, or JP8 (military logistics fuel), make them attractive candidates for portable power. Several of the reformers reviewed successfully processed sulfur-free versions of these fuels. Thus, obviously, a compact sulfur removal system would be of great interest in this area. Larger-scale systems have been developed that rely on absorbents<sup>104</sup> or selective oxidation of the sulfur compounds;<sup>104</sup> however, they tend to be bulky or have other significant limitations. The development of compact, lightweight, desulfurization systems for portable power is a priority for the use of commercially available fuels.

An often neglected area involves BOP components, especially liquid pumps, air blowers or pumps, controls strategy, valves, water management systems, insulation (for both thermal and noise management), sensors, and power conditioning. Developing of low-cost, efficient, reliable, compact blowers and liquid pumps is particularly important for designs that require elevated pressures, such as membrane reactors. The controls strategy and power conditioning are particularly important in developing a safe robust system. Since the fuel cells produce water, a water management system is crucial, especially when the fuel processor and fuel cell system will be operating close to electronic devices. Of course, the BOP needs to be as compact and efficient as possible. Passive BOP systems are preferred; however, active systems may result in significant savings in size and cost. For example, a fuel cell can be designed to be "air breathing", meaning that the cathode air is supplied by natural convection; however, an active design allows the fuel cell to operate at higher power levels, thus reducing the size of the fuel cell (and its associated platinum and other materials costs) and allowing better water management. The developers will need to optimize these systems for their specific applications.

For the highest efficiency to be achieved, the fuel cell and fuel processor must be closely coupled. Several engineering issues need to be resolved. For example, will the anode off-gas be burned in a combustor for the generation of heat; does it contain a high enough heating value to provide the heat; or can the cathode air be used in the combustor, thus eliminating one air blower? Is flow desired first through the combustor or through the fuel cell? What will this do to the system? The answers to these questions will provide the key to optimal integration and packaging. Nontechnical issues such as cost and regulations will also play a role in the success of commercializing the technology. The micropower system (fuel cell, fuel processor, and BOP components) must be competitively priced with appropriately sized alternative primarily batteries. A customer may be willing to spend more to get a better product, but what is the limit? A report prepared by the Darnell Group, Inc., for the U.S. Fuel Cell Council provides interesting insight into this area.<sup>105</sup> As a comparison scenario, they used the introduction of Li-polymer batteries as an alternative to Li-ion batteries. The Li-polymer batteries offered value-added features such as increased robustness and higher specific energy of 145–190 Wh/kg compared to 120–150 Wh/kg for Li-ion batteries,<sup>106</sup> but at a higher cost. The report recounted that the average original equipment manufacturer (OEM) price for a Li-ion battery pack for mobile phones in 1999 was \$13.59, while for a Li-polymer pack it was \$16.39, a price premium of 21%.<sup>105</sup> For notebook computers, the Li-ion battery pack average price to OEMs was \$60.39, and for Li-polymer, it was \$79.77, a price premium of 32%.<sup>105</sup> In 1999, the Li-polymer battery pack prices were expected to decrease by about 14% per year. However, when this decrease did not occur, the Li-polymer battery “failed” in the marketplace as a significant competitor to Li-ion batteries.<sup>105</sup> However, the Darnell Group also reported that major battery manufacturers, Samsung, SDI, LG Chemicals, and SKC, announced in July 2002 they were planning to make “large investments” in Li-polymer battery technology.<sup>105</sup> This announcement was interpreted to mean lower Li-polymer prices, which will then result in lower Li-ion prices.<sup>105</sup> This report demonstrates that (1) while it may be superior, the fuel cell product needs to be priced competitively with its counterpart batteries and (2) the fuel cell product target price needs to be competitive with future, not current, battery prices, and a sharp decrease in battery prices should be anticipated whenever a fuel cell product is introduced.

Government regulations cover a wide range of subjects pertaining to fuel cell systems, such as the fuel cells themselves, fuel packaging, fuel distribution, carrying fuel cells on airplanes, use and transportation of a flammable fuel on airplanes, and fuel processing for portable devices, particularly indoors and especially important for high-pressure applications. These regulations, which can be viewed on government Web sites and obtained from government resources such as the American National Standards Institute (ANSI), the Code of Federal Regulations

(CFR), the International Code Council (ICC), the National Hydrogen Association, and the International Organization for Standardization (ISO), to name a few, will play a part in dictating the expanded use of fuel cell products.

In this paper, hydrogen generation from microreactors was reviewed, design considerations were discussed, fabrication methods were presented, and examples of reactors over a wide power range were examined. It is clear that a great deal of research is occurring in this relatively new area and that impressive progress has been achieved. With the continuing advancements, the future looks bright for this needed technology.

## 5. Acronyms

ATR	autothermal reforming
BOP	balance-of-plant
CFD	computational fluid dynamics
CVD	chemical vapor deposition
DRIE	deep reactive ion etching
EDM	electrodischarge machining
GHSV	gas hourly space velocity
LHV	lower heating value
LIGA	lithographie, galvanofornung, abformtechnik
LTCC	low-temperature co-fired ceramics
MEMS	microelectromechanical systems
PBI	polybenzimidazole
PECVD	plasma enhanced chemical vapor deposition
PEMFC	polymer electrolyte membrane fuel cell
PrOx	preferential oxidation
RF	radio frequency
S/C	steam-to-carbon ratio
SEM	scanning electron microscopy
SLPM	standard liters per minute
SOG	spin-on-glass
STP	standard temperature and pressure
SV	space velocity
TEM	transmission electron microscopy
WGS	water-gas-shift
XRD	X-ray diffraction

## 6. References

- (1) Matta, L. M.; Nan, M.; Davis, S. P.; McAllister, D. V.; Zinn, B. T.; Allen, M. G. American Institute of Aeronautics and Astronautics, Aerospace Sciences Meeting and Exhibit, Reno, NV, 2001; paper 2001-0978.
- (2) Schaevitz, S. B.; Franz, A. J.; Jensen, K. F.; Schmidt, M. A. The 11th International Conference on Solid-State Sensors and Actuators, Munich, Germany, 2001; pp 30–33.
- (3) Fu, K.; Knobloch, A.; Martinez, F.; Walther, D. C.; Fernandez-Pello, C.; Pisano, A. P.; Liepmann, D.; Miyaska, K.; Maruta, K. 2001 International Mechanical Engineering Congress and Exposition, 2001.
- (4) Fu, K.; Knobloch, A. J.; Martinez, F. C.; Walther, D. C.; Fernandez-Pello, C.; Pisano, A. P.; Liepmann, D. 2001 International Mechanical Engineering Congress and Exposition, 2001.
- (5) Maruta, K.; Takeda, K.; Sitzki, L.; Borer, K.; Ronney, P. D.; Wussow, S.; Deutschmann, O. Third Asia-Pacific Conference on Combustion, Seoul, Korea, 2001.
- (6) Richards, C. D.; Bahr, D. F.; Xu, C. G.; Richards, R. F. 36th Intersociety Energy Conversion Engineering Conference, Savannah, GA, 2001.
- (7) Hoogers, G. In *Fuel Cell Technology Handbook*; Hooger, G., Ed.; CRC Press: Boca Raton, FL, 2003.
- (8) Wainright, J. S.; Savinell, R. F. Fall 2000 Meeting of the Electrochemical Society, Phoenix, AZ, 2000.
- (9) Savinell, R. F. Gordon Research Conference on Electrochemistry, CA, 2001.
- (10) Jones, P. B.; Lakeman, J. B.; Mepsted, G. O.; Moore, J. M. *J. Power Sources* **1999**, *80*, 242.
- (11) Oroskar, A. R.; VandenBussche, K. M.; Abdo, S. F. Fifth International Conference on Microreaction Technology, Strasbourg, France, 2001; p 153.

- (12) Henderson, I. R. M. Process Intensification Topical Session in AICHE Spring 2003, New Orleans, LA, 2003; p 109.
- (13) Ehrfeld, W.; Ehrfeld, U. Fifth International Conference on Microreaction Technology, Strausbourg, France, 2001; p 3.
- (14) Wegeng, R. S.; Drost, M. K.; Call, C. J.; Birmingham, J. G.; McDonald, C. E.; Kurath, D. E.; Friedrich, M. U.S. Patent 5,611,214, 1998.
- (15) Wegeng, R. S.; Drost, M. K.; McDonald, C. E. U.S. Patent 5,811,062, 1997.
- (16) Jensen, K. F. *Chem. Eng. Sci.* **2001**, *56*, 293.
- (17) Thompson, L. T. Microreaction Technology and Process Intensification Symposium at the 226th American Chemical Society National Meeting, New York, 2003; abstract 35.
- (18) Johnson, W. L.; Phillips, C. B.; Chen, Z.; Ransom, T. S.; Thompson, L. T. Microreaction Technology and Process Intensification Symposium at the 226th American Chemical Society National Meeting, New York, 2003; abstract number 41.
- (19) Tonkovich, A. Y.; Zilka, J. L.; LaMont, M. J.; Wang, Y.; Wegeng, R. S. *Chem. Eng. Sci.* **1999**, *54*, 2947.
- (20) Ameal, T. A.; Papautsky, I.; Warrington, R. O.; Wegeng, R. S.; Drost, M. K. *J. Propul. Power* **2000**, *16*, 577.
- (21) Xia, Y. N.; Whitesides, G. M. *Angew. Chem., Int. Ed. Engl.* **1998**, *37*, 550.
- (22) Arana, L. R.; Schaevitz, S. B.; Franz, A. J.; Schmidt, M. A.; Jensen, K. F. *J. MEMS* **2003**, *12*, 600.
- (23) Tonkovich, A. L. Y.; Wang, Y.; Gao, Y. U.S. Patent 6,440,895B1, 2002.
- (24) Tonkovich, A. Y.; Perry, S.; Wang, Y.; Rogers, W. A.; Qui, D.; Peng, Y. *Chem. Eng. Sci.*, in press.
- (25) Wan, Y. S. S.; Chau, J. L. H.; Gavriilidis, A.; Yeung, K. L. Fifth International Conference on Microreaction Technology, Strausbourg, France, 2001; p 94.
- (26) Hoogers, G. In *Fuel Cell Technology Handbook*; Hooger, G., Ed.; CRC Press: Boca Raton, FL, 2003.
- (27) *Catalyst Handbook*, 2nd ed.; Twigg, M. W., Ed.; Wolfe Publishing Ltd.: London, 1989.
- (28) Rostrup-Nielsen, J. In *Encyclopedia of Catalysis*; Horvath, I. T., Ed.; Wiley-Interscience, New York, 2003; Vol. 4.
- (29) Trimm, D. L.; Onsan, Z. I. *Catal. Rev.* **2001**, *43*, 31.
- (30) Song, C. S. *Catal. Today* **2002**, *77*, 17.
- (31) Chin, Y. H.; Dagle, R. A.; Dohnalkova, A.; Hu, J.; Wang, Y. *Catal. Today* **2002**, *77*, 79.
- (32) Chin, Y. H.; Wang, Y.; Dagle, R. A.; Li, X. S. *Fuel Process. Technol.* **2003**, *83*, 193.
- (33) Chen, H.; Ouyang, X.; Shin, W. C.; Park, S. M.; Bednarova, L.; Besser, R. S.; Lee, W. Y. IMRET 7, Lausanne, Switzerland, 2003.
- (34) Chen, G.; Yuan, Q.; Li, S.; Pillot, C.; Li, H. Process Intensification—AICHE Spring 2003, New Orleans, LA, 2003; p 21.
- (35) Choi, Y.; Stenger, H. G. *Appl. Catal., B: Environ.* **2002**, *38*, 259.
- (36) Cao, C.; Xia, G.; Holladay, J.; Jones, E.; Wang, Y. *Appl. Catal., A: Gen.* **2004**, *262*, 19.
- (37) Gorecki, B. J.; Haylett, D.; Dietrich, D.; Allen, J. American Institute of Chemical Engineers Topical Proceedings: Fuel Cell Technology: Opportunities and Challenges, New Orleans, LA, 2002; p 136.
- (38) Takezawa, N.; Kobayashi, H.; Hirose, A.; Shimokawabe, M.; Takahashi, K. *Appl. Catal.* **1982**, *4*, 127.
- (39) Iwasa, N.; Takahashi, K.; Masuda, S.; Takezawa, N. *Catal. Lett.* **1993**, *19*, 211.
- (40) Iwasa, N.; Masuda, S.; Ogawa, N.; Takezawa, N. *Appl. Catal.* **1995**, *125*, 145.
- (41) Holladay, J. D.; Jones, E. O.; Phelps, M.; Hu, J. L. *J. Power Sources* **2002**, *108*, 21.
- (42) Pietrogrande, P.; Bezzeccheri, M. In *Fuel Cell Systems*; Blomen, L. J. M. J., Mugerwa, M. N., Eds.; Plenum Press: New York, 1993.
- (43) Adris, A. M.; Pruden, B. B. *Can. J. Chem. Eng.* **1996**, *74*, 177.
- (44) Wang, Y.; Chin, Y.; Rozmiarek, R. T.; Watson, J.; Tonkovich, A. L. Y. *Catal. Today*, in press.
- (45) Wei, J.; Iglesia, E. *J. Phys. Chem. B* **2004**, *108*, 4094.
- (46) Rostrup-Nielsen, J. R. *J. Catal.* **1973**, *31*, 173.
- (47) Ross, J. R. H. In *Surface and Defect Properties of Solids*; Roberts, M. W., Thomas, J. M., Eds.; Chemical Society: London, 1974; Vol. 4.
- (48) Krummenacher, J. J.; West, K. N.; Schmidt, L. D. *J. Catal.* **2003**, *215*, 332.
- (49) Krumpelt, M. Joint DOE/ONR Fuel Cell Workshop, Baltimore, MD, 1999.
- (50) Krumpelt, M.; Krause, T. R.; Carter, J. D.; Kopasz, J. P.; Ahmed, S. *Catal. Today* **2002**, *77*, 3.
- (51) Bellows, R. J. Joint DOE/ONR Fuel Cell Workshop, Baltimore, MD, 1999.
- (52) TeGrotenhuis, W. E.; King, D. L.; Brooks, K. P.; Golladay, B. J.; Wegeng, R. S. 6th International Conference on Microreaction Technology, New Orleans, LA, 2002; p 18.
- (53) Patt, J.; Moon, D. J.; Phillips, C.; Thompson, L. *Catal. Lett.* **2000**, *65*, 193.
- (54) Chandler, B. D.; Schabel, A. B.; Pignolet, L. H. *J. Catal.* **2000**, *193*, 186.
- (55) Hilaire, S.; Wang, X.; Luo, T.; Gorte, R. J.; Wagner, J. *Appl. Catal., A: Gen.* **2001**, *215*, 271.
- (56) Zhao, S.; Gorte, R. J. *Catal. Lett.* **2004**, *92*, 75.
- (57) Wojcik, A.; Middleton, H.; Damopoulos, I.; Van herle, J. *J. Power Sources* **2003**, *118*, 342.
- (58) Gardner, K. 3rd Annual International Symposium on Small Fuel Cells and Battery Technologies for Portable Power Applications, Washington, DC, 2001.
- (59) Uribe, F. A.; Zawodzinski, T. A. 2001 Joint International Electrochemical Society Meeting, San Francisco, CA, 2001; p abs. 339.
- (60) Muradov, N. *J. Power Sources* **2003**, *118*, 320.
- (61) Taylor, J. D.; Herdman, C. M.; Wu, B. C.; Wally, K.; Rice, S. F. *Int. J. Hydrogen Energy* **2003**, *28*, 1171.
- (62) Cortright, R. D.; Davda, R. R.; Dumesic, J. A. *Nature* **2002**, *418*, 964.
- (63) Jones, E.; Holladay, J.; Perry, S.; Orth, R.; Rozmiarek, B.; Hu, J.; Phelps, M.; Guzman, C. E. 5th International Conference on Microreaction Technology, Strausbourg, France, 2001; p 277.
- (64) Holladay, J.; Jones, E.; Palo, D. R.; Phelps, M.; Chin, Y.-H.; Dagle, R.; Hu, J.; Wang, Y.; Baker, E. Materials Research Society 2002 Fall Meeting, Boston, MA, 2002; p FF9.2.
- (65) Holladay, J.; Jones, E.; Phelps, M.; Hu, J. 6th International Conference on Microreaction Technology, New Orleans, LA, 2002; p 107.
- (66) Holladay, J. D.; Jones, E. O.; Phelps, M.; Hu, J. MEMS Components and Applications for Industry, Automobiles, Aerospace, and Communication, Oct 22–23, 2001, San Francisco, CA, 2001; p 148.
- (67) Holladay, J. D.; Palo, D. R.; Dagle, R. A.; Phelps, M. R.; Chin, Y. H.; Wang, Y.; Baker, E. G.; Jones, E. O. *J. Power Sources* **2004**, *131*, 69.
- (68) Holladay, J. D.; Phelps, M. R.; Jones, E.; Palo, D. R. American Institute of Chemical Engineers Topical Conference: Process Intensification, New Orleans, LA, 2003; p 16.
- (69) Holladay, J. D.; Wainright, J. S.; Jones, E. O.; Gano, S. R. *J. Power Sources*, submitted for publication.
- (70) Holladay, J. D.; Palo, D. R.; Dagle, R. A.; Chin, Y. H.; Cao, J.; Xia, G.; Phelps, M.; Wang, Y.; Jones, E.; Baker, E. G. Fuel Cell Seminar 2003, Miami, FL, 2003.
- (71) Bednarova, L.; Chen, H.; Ouyang, X.; Shin, W. C.; Park, S. M.; Besser, R. S.; Lee, W. Y. 3rd International TRI/Princeton Workshop, Princeton, NJ, 2003.
- (72) Bednarova, L.; Ouyang, X.; Chen, H.; Besser, R. S. 226th ACS National Meeting, New York City, New York, 2003.
- (73) Bednarova, L.; Ouyang, X.; Chen, H.; Besser, R. S. 226th ACS National Meeting, New York City, New York, 2003.
- (74) Bednarova, L.; Ouyang, X.; Chen, H.; Lee, W. Y.; Besser, R. S. ACS Symposium 2003, 2003; p 846.
- (75) Besser, R. S.; Lee, W. Y.; Ho, P.; Ouyang, X.; Chen, H.; Bednarova, L. IMRET 7, Lausanne, Switzerland, 2003.
- (76) Besser, R. S.; Shin, W. C. *J. Vac. Sci. Technol., B* **2003**, *21*, 912.
- (77) Ouyang, X.; Chen, H.; Bednarova, L.; Shin, W.; Besser, R. S. To be published in *CEJ*.
- (78) Ouyang, X.; Ho, P.; Chen, H.; Shin, W. C.; Bednarova, L.; Lee, W. Y.; Besser, R. S.; Pau, S.; Pai, C. S.; Taylor, J. A.; Mansfield, W. M. AICHE Annual Meeting 2003, San Francisco, CA, 2003; p Proc. AICHE Annual Meeting.
- (79) Davis, P.; Milliken, J.; Devlin, P.; Gronich, S. 2003 Fuel Cell Seminar, Miami Beach, FL, 2003; p 760.
- (80) Arana, L. R.; Schaevitz, S. B.; Franz, A. J.; Schmidt, M. A.; Jensen, K. F. 6th International Conference on Microreaction Technology, New Orleans, LA, 2002; p 147.
- (81) Quiram, D. J.; Hsing, I.-M.; Franz, A. J.; Jensen, K. F.; Schmidt, M. A. *Chem. Eng. Sci.* **2000**, *55*, 3065.
- (82) Pattekar, A. V.; Kothare, M. V.; Karnik, S. V.; Hatalis, M. K. 5th International Conference on Microreaction Technology, Strausbourg, France, 2001; p 332.
- (83) Karnik, S. V.; Hatalis, M. K.; Kothare, M. V. 5th International Conference on Microreaction Technology, Strausbourg, France, 2001; p 295.
- (84) Karnik, S. V.; Hatalis, M. K.; Kothare, M. V. Materials Science of Microelectromechanical Systems (MEMS) Devices IV, Nov 25–28, 2001, Boston, MA, 2002; p 243.
- (85) Tosti, S.; Bettinali, L.; Violante, V. *Int. J. Hydrogen Energy* **2000**, *25*, 319.
- (86) Li, A.; Liang, W.; Hughes, R. *J. Membr. Sci.* **2000**, *165*, 135.
- (87) Hara, S.; Sakaki, K.; Itoh, N.; Kimura, H.-M.; Asami, K.; Inoue, A. *J. Membr. Sci.* **2000**, *164*, 289.
- (88) Park, G.-G.; Seo, D. J.; Park, S.-H.; Yoon, Y.-G.; Kim, C.-S. *Chem. Eng. J.*, submitted for publication.
- (89) Palo, D. R.; Holladay, J. D.; Dagle, R. A.; Chin, Y. H.; Baker, E. G. American Institute of Chemical Engineers: 2nd Topical Conference on Fuel Cell Technology, New Orleans, LA, 2003; p 143.
- (90) Palo, D. R.; Holladay, J. D.; Rozmiarek, R. T.; Guzman-Leong, C. E.; Wang, Y.; Hu, J.; Chin, Y. H.; Dagle, R. A.; Baker, E. G. 5th International Conference on Microreaction Technology, Strausbourg, France, 2001; p 359.

- (91) Palo, D. R.; Holladay, J. D.; Rozmiarek, R. T.; Guzman-Leong, C. E.; Wang, Y.; Hu, J. L.; Chin, Y. H.; Dagle, R. A.; Baker, E. G. *J. Power Sources* **2002**, *108*, 28.
- (92) Delsman, E. R.; Rebrov, E. V.; de Croon, M. H. J. M.; Schouten, J. C.; Kramer, G. J.; Cominos, V.; Richter, T.; Veenstra, T. T.; van den Berg, A.; Cobden, P. D.; F. A., d. B.; D'Ortona, U.; Falk, L. 5th International Conference on Microreaction Technology, Strasbourg, France, 2001; p 368.
- (93) Cominos, V.; Hardt, S.; Hessel, V.; Kolb, G.; Löwe, H.; Wichert, M.; Zapf, R. 6th International Conference on Microreaction Technology, New Orleans, LA, 2002; p 113.
- (94) Changrani, R.; Gervasio, D.; Koripella, R.; Rogers, S. P.; Samms, S. R.; Tasic, S. 6th International Conference on Microreaction Technology, New Orleans, LA, 2002; p 108.
- (95) Call, C. J.; Powell, M. R.; Fountain, M.; Chellappa, A. S. The Knowledge Foundation's 3rd Annual International Symposium on Small Fuel Cells and Battery Technologies for Portable Power Applications, Washington, DC, 2001.
- (96) Chellappa, A. S.; Powell, M. R.; Fountain, M.; Call, C. J.; Godshall, N. A. *Abstr. Pap. Am. Chem. Soc.* **2002**, *224*, 123-FUEL.
- (97) Ledjeff-Hey, K.; Formanski, V.; Kalk, T.; Roes, J. *J. Power Sources* **1998**, *71*, 199.
- (98) Ledjeff-Hey, K.; Kalk, T.; Mahlendorf, F.; Niemzig, O.; Trautmann, A.; Roes, J. *J. Power Sources* **2000**, *86*, 166.
- (99) Pfeifer, P.; Fichtner, M.; Schubert, K.; Liauw, M. A.; Emig, G. 3rd International Conference on Microreaction Technology, Frankfurt, Germany, 1999.
- (100) Pfeifer, P.; Schubert, K.; Fichtner, M.; Liauw, M. A.; Emig, G. 6th International Conference on Microreaction Technology, New Orleans, LA, 2002; p 125.
- (101) Thurgood, C. P.; Amphlett, J. C.; Mann, R. F.; Peppley, B. A. 2nd Topical Conference on Fuel Cell Technology, 2003 Spring AICHE National Meeting, New Orleans, LA, 2003; p 161.
- (102) Wheeldon, I. R.; Amphlett, J. C.; Mann, R. F.; Peppley, B. A.; Thurgood, C. P. 2nd Topical Conference on Fuel Cell Technology, 2003 Spring AICHE National Meeting, New Orleans, LA, 2003; p 156.
- (103) Amphlett, J. C.; Mann, R. F.; Peppley, B. A.; Stokes, D. M. Proceedings of the 26th Intersociety Energy Conversion Engineering Conference—IECEC '91, Aug 4–9, 1991, Boston, MA, 1991; p 642.
- (104) Lampert, J. Eighth Grove Fuel Cell Symposium, London, England, 2003; p O2B.5.
- (105) *Fuel Cells for Portable Power: Markets, Manufacture and Cost*; Darnell Group Inc.: 2003.
- (106) Ehrlich, G. M. In *Handbook of Batteries*, 3rd ed.; Linden, D., Reddy, T. B., Eds.; McGraw-Hill: New York, 2002.

CR020721B

